PHYSICAL REVIEW E, VOLUME 63, 046702

# Quantum lattice-gas model for computational fluid dynamics

Jeffrey Yepez*
*Air Force Research Laboratory, Hanscom Air Force Base, Massachusetts 01731*
(Received 2 December 1999; revised manuscript received 15 November 2000; published 29 March 2001)

Quantum-computing ideas are applied to the practical and ubiquitous problem of fluid dynamics simulation. Hence, this paper addresses two separate areas of physics: quantum mechanics and fluid dynamics (or specifically, the computational simulation of fluid dynamics). The quantum algorithm is called a *quantum lattice gas*. An analytical treatment of the microscopic quantum lattice-gas system is carried out to predict its behavior at the mesoscopic scale. At the mesoscopic scale, a lattice Boltzmann equation with a nonlocal collision term that depends on the entire system wave function, governs the dynamical system. Numerical results obtained from an exact simulation of a one-dimensional quantum lattice model are included to illustrate the formalism. A symbolic mathematical method is used to implement the quantum mechanical model on a conventional workstation. The numerical simulation indicates that classical viscous damping is not present in the one-dimensional quantum lattice-gas system.

DOI: 10.1103/PhysRevE.63.046702 PACS number(s): 47.11.+j, 03.67.Lx, 05.60.Gg

## I. INTRODUCTION

### A. Overview

The purpose of this paper is to show that a phase-coherent quantum computer can be used to simulate the behavior of a system of massive quantum particles, propagating and colliding on a discrete space-time lattice. This discrete quantum particle system is called a *quantum lattice gas*. I have used principles and concepts from quantum mechanics instead of from classical mechanics to formulate "local rules" for an artificial microscopic particle dynamics. In a quantum lattice gas, this is possible because a network of two-energy-level quantum systems is used to encode the configuration of particle occupancies throughout the lattice.

There are two parts to this paper. First, I analyze a globally phase-coherent and entangled quantum lattice-gas system governed by the many-body Schrödinger equation of quantum mechanics.[1] The many-body Schrödinger equation is reformulated as a Boltzmann equation of kinetic transport. Assuming the quantum computer's wave function does not decohere by uncontrolled entanglement with the external world, the main analytical result of this paper is the derivation of a lattice Boltzmann equation that exactly describes kinetic transport at the mesoscopic scale in the quantum lattice gas. That is, the lattice-Boltzmann equation is an exact representation of the particle dynamics, including all effects due to quantum superposition and entanglement. This reformulation of many-body quantum mechanics represents a quantum computing application geared towards the direct simulation of physical dynamical models. A hydrodynamic fluid simulation is considered here as a test case.

Second, numerical data taken from an exact simulation of a globally phase-coherent quantum lattice-gas system is presented. The simulation method uses symbolic mathematics to implement a quantum mechanical system in the second quantized representation. A globally phase-coherent wave function is simulated on a classical computer. This is possible because the number of spatial sites of the lattice is small and the number of qubits per site is few. The main finding from the simulation is that it is possible for mass-density waves to oscillate indefinitely. The simulation confirms that there is no viscous damping in the hydrodynamic sound mode of the artificial fluid.

### B. Background

Other types of quantum lattice gases have been studied, beginning in the mid 1990s, by Bialynicki-Birula [1], Succi [2,3], Meyer [4,5], and Boghosian and Taylor [6] to model the relativistic Dirac equation and the nonrelativisitic Schrödinger equation. In contrast, the macroscopic scale behavior of the quantum lattice gas presented here is classical, even though the microscopic scale dynamics is quantum mechanical rather than classical in nature. The quantum lattice gas reduces to a classical lattice gas only if the collision process causes a particular incoming configuration of particles to scatter into only one single "outgoing" configuration.[2]

In two previous papers on quantum lattice gases [7,8], I considered a quantum spin system where the system wave function was collapsed into a tensor product state over the spins (or qubits) after each collision step. This allows for local entanglement to occur temporarily and avoids global entanglement altogether when the particles propagate through the lattice [7]. Allowing for only short-range and short-time entanglement of qubits, the quantum lattice-gas system is described at the mesoscopic scale by a lattice Boltzmann equation, with a local collision operator that obeys the principle of detailed balance [8] (we may refer to this model as a *factorized quantum lattice gas*). It provides a

*Email address: Jeffrey.Yepez@hanscom.af.mil; URL:http://xyz.plh.af.mil

[1]The quantum state of the quantum lattice gas is said to be *globally entangled* when qubits in the system are entangled with other qubits in the system positioned arbitrarily far away in the lattice.

[2]This follows since it is a direct generalization of a classical lattice gas with quantum bits replacing classical bits.

way to implement the lattice Boltzmann equation in an unconditionally stable manner on a classical computer. Although quantum mechanical ideas inspired the formulation of the collision process, in the end, the factorized quantum lattice gas is a probabilistic classical process. The salient feature of the factorized quantum lattice-gas formulation is that it is suited for implementation on an array of small quantum computers, interconnected by a classical communication network. Therefore, the previous papers do not address the situation where quantum superposition and entanglement can spread throughout the entire quantum computer. This situation is treated here.

### C. Organization

In Sec. II, I introduce the *quantum lattice-gas formulation* from an analytical perspective. The quantum lattice gas is treated at the microscopic and mesoscopic scales in Secs. II A and II B, respectively. When the quantum computer is fully coherent throughout the entire course of the simulation, the collision operator is nonlocal. Evaluating it requires knowledge of the entire system wave function on the quantum computer. An exact representation of the quantum lattice gas' mesoscopic behavior is developed in Sec. II B. Its mesoscopic behavior is governed by a lattice-Boltzmann equation.

The quantum lattice-gas formalism is presented from a numerical perspective in Sec. III. The numerical methodology used in the simulation of the quantum system is presented in Sec. III A. The numerical method discussed in Sec. III A 1 is based on a representation of a universal quantum gate expressed in terms of the creation and annihilation operators. The symbolic rules used to carry out the exact simulation is described in Sec. III A 2. A simple one-dimensional lattice-gas model, used in this paper for test purposes, is described in Sec. III B. I have included various computer simulations with both classical and quantum mechanical microscopic dynamics. The classical and quantum mechanical versions of this simple one-dimensional lattice-gas model, called the *1D3Px model*, are described in Secs. III B 1 and III B 2, respectively. Simulation results are presented in Sec. III C. The classical and quantum mechanical simulations results are presented in Secs. III C 1 and III C 2, respectively. The classical simulations, provided for comparison purposes, are done at the microscopic scale and also in a classical mesoscopic mean-field approximation. Then, I present an exact simulation of the quantum 1D3Px model, with three qubits per site for small systems. Approximation schemes are needed to compute the many-body dynamics on a classical computer, except in the case of very small system size or systems with very few particles. An exact quantum simulation of a small cluster, comprising 21 qubits, is carried out on a conventional workstation using a symbolic mathematics technique that is described in Sec. III A. The numerical simulation gives us a way to understand the quantum lattice-gas method in concrete terms and is a necessary step toward achieving numerical simulations on quantum computers.

A brief summary of the results and a few closing remarks are given in Sec. IV.

## II. ANALYTICAL TREATMENT

### A. Microscopic scale

In quantum computing [9,10], a two-level quantum bit (called a *qubit*) represents the smallest unit of information that may be in a superposition of the discrete states $|0\rangle$ and $|1\rangle$. A qubit $|q\rangle=\alpha|0\rangle+\beta|1\rangle$ has an amplitude $\alpha$ of being in the *zero state*, $|0\rangle$, and another amplitude $\beta$ of being in the *one state*, $|1\rangle$. The complex coefficients are constrained by $|\alpha|^2+|\beta|^2=1$ so that the probability of the qubit being in the zero state plus the probability of it being in the one state is unity. For any unitary quantum computation, one can describe the algorithm by specifying a unitary evolution operation, in our case formally written as $e^{i\hat{H}\tau/\hbar}$, acting on the system wave function, $|\Psi(t)\rangle$, which constitutes the state of the quantum computer's "memory." With $N$ qubits, the quantum state $|\Psi(t)\rangle$ resides in a large Hilbert space with $2^N$ dimensions. A new quantum state $|\Psi(t+\tau)\rangle$ is generated by application of a unitary operator (which could be represented by a unitary matrix of size $2^N\times 2^N$) for a short duration $\tau$ as

$$|\Psi(t+\tau)\rangle=e^{i\hat{H}\tau/\hbar}|\Psi(t)\rangle. \tag{2.1}$$

By repeated application of $e^{i\hat{H}\tau/\hbar}$, an ordered sequence of states is generated and each one is given a unique time label. If the first state is labeled by $t$ then the next one is labeled by $t+\tau$, and the next by $t+2\tau$, and so forth. In this way, think of the *computational time* advancing incrementally in unit steps of duration $\tau$. Of course the state of the quantum computer exists at all intermediate times, say at $t+\tau/2$, but for our purposes we need to consider only the state at intervals of the time step $\tau$. Formally, the quantum computer's evolution is invertible by application of the adjoint of the evolution operator

$$|\Psi(t-\tau)\rangle=e^{-i\hat{H}\tau/\hbar}|\Psi(t)\rangle. \tag{2.2}$$

This computational picture is consistent with the Heisenberg picture of quantum mechanics. For any reversible algorithm chosen, the task is to map the algorithm onto the dynamical evolution of interacting qubits within the physical device, which can be driven by external control.

#### *1. Preliminaries*

Consider a quantum computer with qubits arranged in a lattice-based array with the following properties:

(1) $V$ is the number of lattice sites.

(2) $B$ is the number of qubits per site (and the number of nearest neighbors).

(3) $N=VB$ is the total number of qubits.

(4) $2^N$ is the size of the full Hilbert space.

(5) $2^B$ is the size of the on-site submanifold, denoted $\mathcal{B}$ (and the number of on-site configurations).

TABLE I. Ket symbols.

| Symbol | Size of manifold | Description |
|---|---|---|
| $\|\Psi\rangle$ | $2^N$ | Total system ket |
| $\|\psi\rangle$ | $2^B$ | On-site ket |
| $\|q\rangle$ | 2 | Qubit, local state ket |

At each site of the lattice resides a group of qubits acted upon by a sequence of *quantum gates* [10–13], whose action is mediated by external control. The quantum lattice gas' evolution can be formally expressed as a special case of Eq. (2.1) where $e^{iH\tau/\hbar} \equiv \hat{S}\hat{C}$ as follows:

$$|\Psi(\vec{x}_1, \ldots, \vec{x}_V; t+\tau)\rangle = \hat{S}\hat{C}|\Psi(\vec{x}_1, \ldots, \vec{x}_V; t)\rangle. \quad (2.3)$$

In Eq. (2.3), $\hat{S}$ is the *streaming* operator, which in matrix representation is an orthogonal permutation matrix with components being either 0 or 1. $\hat{S}$ is the "classical" lattice-gas streaming operator. However, in Eq. (2.3), $\hat{C}$ is not a classical operator. It is a unitary *collision* operator. In general, when expressed in matrix form, $\hat{C}$ has complex components. (The quantum lattice gas reduces to a deterministic classical lattice gas if $\hat{C}$ is a permutation matrix with 0 or 1 components. If and when $\hat{C}$ is stochastically switched between different permutation matrices during the dynamical evolution, then the quantum lattice gas reduces to a probabilistic classical lattice gas.) Finally, in Eq. (2.3), I have explicitly labeled the wave function's dependence on all the coordinates of the lattice to emphasize that the wave function is a lattice-based field quantity.

In general, the operator $\hat{C}$ can cause mixing of outgoing collisional configurations at each site of the lattice, locally entangling the qubit states within a lattice cell of size $\ell$. The operator $\hat{S}$ then causes particles to move from one site to the next, by exchanging qubit states between nearest neighboring sites. Although the application of $\hat{S}$ causes the particles to move just as they would in the streaming phase of a classical lattice gas, it also causes global superposition and entanglement of all the qubit states, if local entanglement has already been caused by $\hat{C}$. In this way, quantum entanglements are spread throughout the lattice by the action of $\hat{S}$.

I will use the following convention for indices.

(1) Small roman letters $(a,b,c)$ for the momentum directions on the lattice, $a \in \{0, \ldots, B-1\}$.

(2) Greek letters $(\alpha,\beta,\gamma)$ for specifying qubits, $\alpha \in \{0, \ldots, N-1\}$.

(3) Middle roman letters $(i,j,k)$ for the spatial dimensions, $i \in \{1, \ldots, D\}$.

### 2. System wave function

Let $|\Psi\rangle$, $|\psi\rangle$, and $|q\rangle$ denote the *total system ket*, *on-site ket*, and *qubit ket*, repectively, as shown in Table I. The quantum computer's total wave function can in general be expressed as a linear combination of tensor product states over all the qubits

$$|\Psi(\vec{x}_1, \ldots, \vec{x}_V; t)\rangle = \sum_{\{q_1, \ldots, q_N\}} A(q_1, \ldots, q_N) \times |q_1\rangle \otimes \cdots \otimes |q_N\rangle. \quad (2.4)$$

Here the summation indices $q_\alpha$ are either zero or one, for $1 \leq \alpha \leq N$. Each tensor product $|q_1\rangle \otimes \cdots \otimes |q_N\rangle$ is a basis state and $|\Psi\rangle$ is a pure classical state. The number representation (2.4) is used in the numerical quantum simulation presented in Sec. III C. I would like to establish a convention for representing the system ket as a linear combination of tensor product states that are lattice-site specific. Let $|\psi\rangle$ denote an *on-site ket* formed over the qubits at a single site of the lattice

$$|\psi(\vec{x},t)\rangle = \sum_{\{q_1, \ldots, q_B\}} a(q_1, \ldots, q_B) \times |q_1(\vec{x},t)\rangle \otimes \cdots \otimes |q_B(\vec{x},t)\rangle. \quad (2.5)$$

The system wave function (2.4) can in general also be expressed as a linear combination of tensor product states over all the on-site kets

$$|\Psi(\vec{x}_1, \ldots, \vec{x}_V; t)\rangle = \sum_{\{\psi_1, \ldots, \psi_V\}} \mathcal{A}(\psi_1, \ldots, \psi_V) \times |\psi_1\rangle \otimes \cdots \otimes |\psi_V\rangle, \quad (2.6)$$

where the shorthand notation $|\psi_n\rangle \equiv |\psi(\vec{x}_n, t)\rangle$ is used. Here the indices $\psi_n$ (for $1 \leq n \leq V$) in the sum represent the numbered basis states in the on-site manifold $\mathcal{B}$. So they are in the range $0 \leq \psi_n \leq 2^B - 1$. The coefficients $\mathcal{A}$ account for all the global superpositions between lattice sites.

### 3. Unitary collision matrix

Collisions are implemented independently at each site of the lattice. Hence, all sites can be collided in parallel, homogeneously across the entire system. The collision operator $\hat{C}$ is therefore expressible in tensor product form since local quantum superposition of outgoing on-site configurations occurs only within each $2^B$-dimensional submanifold $\mathcal{B}$. The $2^N \times 2^N$ collision matrix $\hat{C}$ can be written as the following tensor product:

$$\hat{C} = \bigotimes_{x=1}^{V} \hat{U}, \quad (2.7)$$

where the *on-site collision matrix* $\hat{U}$ is a $2^B \times 2^B$ unitary matrix. It acts on the on-site ket

$$|\psi'(\vec{x},t)\rangle = \hat{U}|\psi(\vec{x},t)\rangle. \quad (2.8)$$

The prime on the left-hand side (LHS) of Eq. (2.8) indicates that the ket is an *outgoing* collisional state. Using the representation (2.6) of the system ket, the postcollision system ket is

$$|\Psi'(\vec{x}_1,\ldots,\vec{x}_V;t)\rangle=\hat{C}|\Psi(\vec{x}_1,\ldots,\vec{x}_V;t)\rangle$$
$$=\sum_{\{\psi_1,\ldots,\psi_V\}}\mathcal{A}(\psi_1,\ldots,\psi_V)\hat{U}$$
$$\times|\psi_1\rangle\otimes\cdots\otimes\hat{U}|\psi_V\rangle$$
$$=\sum_{\{\psi_1',\ldots,\psi_V'\}}\mathcal{A}'(\psi_1',\ldots,\psi_V')$$
$$\times|\psi_1'\rangle\otimes\cdots\otimes|\psi_V'\rangle. \quad (2.9)$$

An *equivalence class* is defined as a set of basis states that correspond to particle configurations with the same mass and momentum (and energy if that is also defined in the lattice-gas model). The on-site unitary collision operator $\hat{U}$ acting on the $\mathcal{B}$-submanifold itself is block diagonal over the equivalence classes. Consider, for example, the quantum 1D3Px lattice gas (see Sec. III B 1 for a detailed description of the 1D3Px lattice-gas model). There are two conserved quantities for this one-dimensional system: the mass and the momentum along the $x$ axis. Hence, there is only one equivalence class and it has two members, a two-body head-on configuration and a configuration with a single rest particle. Both configurations have $m=2$ and $\vec{p}=0$. The equivalence class is comprised of the following on-site kets:

$$|3\rangle=|011\rangle,$$

$$|4\rangle=|100\rangle.$$

A general outgoing ket in this mass-momentum sector of the on-site submanifold is a linear combination of these two,

$$\alpha|011\rangle+\beta|100\rangle, \quad (2.10)$$

where $\alpha$ and $\beta$ are complex numbers. So the collision matrix $\hat{U}$ for this one-dimensional quantum lattice gas has one block. It has a $2\times2$ block for mixing the head-on and rest particle configurations. In general, $\hat{U}$ is block diagonal over the equivalence classes [7]. Each block of $\hat{U}$, associated with an equivalence class of size $n$, is a member of the $U(n)$ unitary group.

### B. Mesoscopic scale

#### 1. Occupancy probability and the mass and momentum densities

The *probability of occupancy* at time $t$ of the $\alpha$th local state is denoted $f_\alpha(t)$. Let the $\alpha$th local state be associated with a displacement vector $\hat{e}_a$ at position $\vec{x}$. Also, let $\hat{n}_\alpha$ denote the number operator for the $\alpha$th local state. That is, $\hat{n}_\alpha|\Psi(t)\rangle$ has eigenvalue 1 or 0 corresponding to the $\alpha$th local state being occupied or empty at time $t$. A fundamental construct of the quantum lattice-gas formalism is that the probability of occupancy $f_\alpha(t)$ is expressed in terms of the quantum mechanical density matrix $\varrho(t)=|\Psi(t)\rangle\langle\Psi(t)|$ as the following trace:

$$f_\alpha(t)=f_a(\vec{x},t)\equiv\mathrm{Tr}[\varrho(t)\hat{n}_\alpha]. \quad (2.11)$$

In the literature on classical lattice gases and the lattice-Boltzmann equation, $f_a(\vec{x},t)$ is referred to as the *single-particle distribution function*, and it is defined at the mesoscopic scale. For classical lattice gases, numerical estimates of $f_a(\vec{x},t)$ are obtained either by ensemble averaging over many independent microscopic systems or by coarse-grain averaging over space-time blocks with a single microscopic system. For the quantum lattice gas, the $f_a(\vec{x},t)$ is the expectation value of the operator $\hat{n}_\alpha$ determined by repeated measurement of single microscopic realizations or by direct measurement of an ensemble, as occurs in nuclear magnetic resonance quantum computers [14,15]. So the definition (2.11) also defines $f_a(\vec{x},t)$ at the mesoscopic scale.

Let $\alpha_\mathrm{O}$ denote the first local state within the group of local states at position $\vec{x}$ of the Bravais lattice. In addition, let $\alpha_\mathrm{O}$ correspond to the displacement vector $\hat{e}_0$. Next, suppose the local states are numbered in a systematic and well-ordered fashion so that each local state $\alpha=\alpha_\mathrm{O}+a$, for all $a\in\{0,1,\ldots,B-1\}$, resides at position $\vec{x}$. Note that with this numbering scheme, the directional index $a$, associated with the $\alpha$th local state, is found by the modulus operation $a=(\alpha \bmod B)$. Then, the local mass density and the momentum density at $\vec{x}$ and $t$ can be expressed in terms of the occupancy probability $f_a(\vec{x},t)$ following the convention used to define the mass and momentum densities in a classical lattice gas

$$\rho(\vec{x},t)=\lim_{\ell_s\to0}\sum_{a=1}^{B}m f_a(\vec{x},t)=\lim_{\ell\to0}\sum_{\alpha=\alpha_\mathrm{O}}^{\alpha_\mathrm{O}+B}m\,\mathrm{Tr}[\varrho(t)\hat{n}_\alpha], \quad (2.12)$$

$$\rho(\vec{x},t)v_i(\vec{x},t)=\lim_{\ell_s\to0}\sum_{a=1}^{B}mc^2e_{ai}f_a(\vec{x},t)$$
$$=\lim_{\ell\to0}\sum_{\alpha=\alpha_\mathrm{O}}^{\alpha_\mathrm{O}+B}mc^2e_{(\alpha \bmod B)i}\mathrm{Tr}[\varrho(t)\hat{n}_\alpha]. \quad (2.13)$$

The mass and momentum densities are considered "macroscopic" field quantities. They are only well defined in the *continuum limit*, where the primitive cell size of the lattice approaches zero. However, for practical considerations, they are approximated by high resolution grids with small but finite cell size.

To experimently determine the mass density or momentum density at a site $\vec{x}$ at time $t$ in an actual quantum system, it is necessary to know the probability of occupancy of all the local states at that site $f_a(\vec{x},t)$ for $a=1,\ldots,B$, according to the definitions (2.12) and (2.13). The probability of occupancy $f_a(\vec{x},t)$ of each local state depends on the polarization of the corresponding qubit $|q_a(\vec{x},t)\rangle=\alpha_a(\vec{x},t)|0\rangle+\beta_a(\vec{x},t)|1\rangle$. A Von Neuman measurement of the state of

TABLE II. Two neighboring qubits.

| Qubits | $\|q\rangle$ | $\|q'\rangle$ |
|---|---|---|
| Local state | $\alpha$ | $\alpha'$ |
| Position | $\vec{x}$ | $\vec{x}'=\vec{x}+\ell\hat{e}_a$ |
| Momentum | $\vec{p}=mc\hat{e}_a$ | $\vec{p}'=\vec{p}$ |

this qubit will yield a value of either 0 or 1, with probability $|\alpha_a(\vec{x},t)|^2$ or $|\beta_a(\vec{x},t)|^2$, respectively, since the measurement causes a collapse of the quantum wave function. A single value obtained by this stochastic measurement process is not sufficient to determine $f_a(\vec{x},t)$. Therefore, to obtain an estimate of the expected equilibrium values of the mass and momentum densities, it is necessary to either ensemble average over many realizations of the microscopic system or coarse-grain average over space-time blocks within a single microscopic realization. In this regard, the amount of effort needed to obtain estimates of the densities is identical for the quantum system and classical lattice-gas sysytems. A quantum computer that provides a direct means for measuring the expected state of a qubit (such as is possible with an NMR quantum computer) would be a more natural choice for implementing this quantum lattice-gas algorithm.

If measurements were made at each and every site, and at every time step of the dynamics, then the quantum lattice-gas system is effectively "factorized" in such a way that the quantum computer's wave function is always collapsed into a tensor product state. This type of factorized quantum lattice-gas simulation, with continual and homogeneous measurement of the qubits, results in a probabilistic classical lattice-gas simulation [8]. Yet, even in this case, the value of the transport coefficients can differ from those of the classical lattice gas.

### *2. Mesoscopic transport equation*

Let us consider two qubits $|q\rangle$ and $|q'\rangle$, which are located at neighboring sites $\vec{x}$ and $\vec{x}'=\vec{x}+\ell\hat{e}_a$, respectively. I shall refer to the local states encoded by these two neighboring qubits by their numerical labels $\alpha$ and $\alpha'$, respectively. Next, suppose these local states may be occupied by particles with momentum $mc\hat{e}_a$. Following this construction, the action of the streaming operator $\hat{S}$ causes a particle to move from site $\vec{x}$ to the neighboring site $\vec{x}'$, hopping from local state $\alpha$ with momentum $\vec{p}=mc\hat{e}_a$ to local state $\alpha'$ with the same momentum $\vec{p}'=\vec{p}$. This labeling convention is summarized in Table II. With this understanding, we can write the identity.

$$\langle\Psi|\hat{n}_\alpha|\Psi\rangle=\langle\Psi|\hat{S}^\dagger\hat{n}_{\alpha'}\hat{S}|\Psi\rangle. \tag{2.14}$$

This is a simple mathematical way of stating the following: If you make a measurement of the occupancy of local state $\alpha$ before streaming, the result you get must be the same as when you make a measurement of $\alpha'$ after streaming.

The first step toward deriving a microscopic transport equation for the quantum lattice gas is to rewrite Eq. (2.3) as

$$\langle\Psi(t)|\hat{C}^\dagger\hat{n}_\alpha\hat{S}^\dagger|\Psi(t+\tau)\rangle=\langle\Psi(t)|\hat{C}^\dagger\hat{n}_\alpha\hat{C}|\Psi(t)\rangle, \tag{2.15}$$

which is done by multiplying through from the left by $\langle\Psi(t)|\hat{C}^\dagger\hat{n}_\alpha\hat{S}^\dagger$, and then using the identity $\hat{S}^\dagger\hat{S}=\mathbf{1}$. From the identity (2.14), we know that $\hat{n}_\alpha\hat{S}^\dagger=\hat{S}^\dagger\hat{n}_{\alpha'}$. Using this fact in the above equation allows us to write it as

$$\langle\Psi(t)|\hat{C}^\dagger\hat{S}^\dagger\hat{n}_{\alpha'}|\Psi(t+\tau)\rangle=\langle\Psi(t)|\hat{C}^\dagger\hat{n}_\alpha\hat{C}|\Psi(t)\rangle. \tag{2.16}$$

The "bra" vector on the LHS of this equation can be simplified using the adjoint of Eq. (2.3), which is $\langle\Psi(t+\tau)|=\langle\Psi(t)|\hat{C}^\dagger\hat{S}^\dagger$, so that we obtain the following result:

$$\langle\Psi(t+\tau)|\hat{n}_{\alpha'}|\Psi(t+\tau)\rangle=\langle\Psi(t)|\hat{C}^\dagger\hat{n}_\alpha\hat{C}|\Psi(t)\rangle. \tag{2.17}$$

Using Eq. (2.11) and referring to Table II, Eq. (2.17) expresses the probability of occupancy of local state $\alpha'$ at site $\vec{x}+\ell_s\hat{e}_a$ at time $t+\tau$ in terms of a matrix element evaluated at the neighboring site $\vec{x}$ and at the earlier time $t$. That is,

$$f_a(\vec{x}+\ell_s\hat{e}_a,t+\tau)=\langle\Psi(t)|\hat{C}^\dagger\hat{n}_\alpha\hat{C}|\Psi(t)\rangle. \tag{2.18}$$

We may add $f_a(\vec{x},t)-\langle\Psi(t)|\hat{n}_\alpha|\Psi(t)\rangle$, which vanishes by definition, to the right-hand side (RHS) of Eq. (2.18). Then, we recognize Eq. (2.18) is a transport equation for the particle occupancies. The result is a lattice-Boltzmann equation for the quantum lattice-gas system

$$f_a(\vec{x}+\ell_s\hat{e}_a,t+\tau)=f_a(\vec{x},t)+\Omega_a^{\text{meso}}(\Psi), \tag{2.19}$$

where the collision term is expressed as the following matrix element:

$$\Omega_a^{\text{meso}}(\Psi)\equiv\langle\Psi(t)|\hat{C}^\dagger\hat{n}_\alpha\hat{C}-\hat{n}_\alpha|\Psi(t)\rangle. \tag{2.20}$$

An alternative derivation of Eq. (2.20), carried out in the continuum limit, is given in Appendix A. In practice, we will not be able to analytically evaluate Eq. (2.20) for a large quantum lattice-gas system with global entanglement because of the exponential size of the $|\Psi\rangle$ ket. However, it is possible to formally express the collision term $\Omega_a^{\text{meso}}$ when $|\Psi\rangle$ is represented as the linear combination (2.6). This is done as follows:

$$\begin{aligned}\Omega_a^{\text{meso}}=&\sum_{\{\psi_{1'},\ldots,\psi_{V'}\}}\sum_{\{\psi_1,\ldots,\psi_V\}}\mathcal{A}^*(\psi_{1'},\ldots,\psi_{V'})\\&\times\mathcal{A}(\psi_1,\ldots,\psi_V)\langle\psi_{1'}|\otimes\cdots\\&\otimes\langle\psi_{V'}|\hat{C}^\dagger\hat{n}_\alpha\hat{C}-\hat{n}_\alpha|\psi_1\rangle\otimes\cdots\otimes|\psi_V\rangle.\end{aligned} \tag{2.21}$$

Moreover, it is possible to express $\Omega_a^{\text{meso}}$ in terms of the on-site number operator $\hat{n}_a$, which is represented by a $2^B\times2^B$ matrix. That is, $\hat{n}_a$ acts only in the submanifold $\mathcal{B}$ on the qubits at a single site. We write the $N$-qubit number operator $\hat{n}_\alpha$ as a $V$-fold tensor product that has a single

$B$-qubit number operator $\hat{n}_a$ located at the $n$th site index corresponding to the position vector $\vec{x}_n$ as

$$\hat{n}_a = \mathbf{1}\otimes\mathbf{1}\otimes\cdots\otimes\hat{n}_a\otimes\cdots\otimes\mathbf{1}, \tag{2.22}$$

where $\mathbf{1}$ denotes the $2^B\times 2^B$ identity matrix. The collision operator $\hat{C}^\dagger\hat{n}_a\hat{C}-\hat{n}_a$, can then be written as

$$\mathbf{1}\otimes\mathbf{1}\otimes\cdots\otimes(\hat{U}^\dagger\hat{n}_a\hat{U}-\hat{n}_a)\otimes\cdots\otimes\mathbf{1}=\otimes_{x=1}^{V}\hat{\Omega}_a, \tag{2.23}$$

where

$$\hat{\Omega}_a\equiv\begin{cases}\hat{U}^\dagger\hat{n}_a\hat{U}-\hat{n}_a, & x=x_n\\ \mathbf{1}, & \text{otherwise.}\end{cases} \tag{2.24}$$

Using Eqs. (2.7), (2.22), and the orthonormality of the on-site kets $\langle\psi_{n'}|\psi_n\rangle=\delta_{n'n}$, Eq. (2.21) reduces to a local matrix element evaluated at single site $\vec{x}_{n'}=\vec{x}_n=\vec{x}$ as

$$\begin{aligned}\Omega_a^{\text{meso}}=&\sum_{\psi_{n'}}\sum_{\{\psi_1,\ldots,\psi_V\}}\\ &\times\mathcal{A}^*(\psi_1,\ldots,\psi_{n-1},\psi_{n'},\psi_{n+1},\ldots,\psi_V)\\ &\times\mathcal{A}(\psi_1,\ldots,\psi_n,\ldots,\psi_V)\langle\psi_{n'}|\hat{U}^\dagger\hat{n}_a\hat{U}-\hat{n}_a|\psi_n\rangle.\end{aligned} \tag{2.25}$$

Let us make the following definition:

$$\begin{aligned}\mathcal{R}(\psi_{n'},\psi_n)\equiv&\sum_{\{\psi_1,\ldots,\psi_{n-1},\psi_{n+1},\ldots,\psi_V\}}\\ &\times\mathcal{A}^*(\psi_1,\ldots,\psi_{n-1},\psi_{n'},\psi_{n+1},\ldots,\psi_V)\\ &\times\mathcal{A}(\psi_1,\ldots,\psi_n,\ldots,\psi_V).\end{aligned} \tag{2.26}$$

The quantity $\mathcal{R}(\psi_{n'},\psi_n)$ represents the superposition of the on-site basis states at site $\vec{x}$ with all the other on-site basis states in the system at the other sites. With this definition, Eq. (2.25) can be written in a simpler way,

$$\Omega_a^{\text{meso}}=\sum_{\psi_{n'}}\sum_{\psi_n}\mathcal{R}(\psi_{n'},\psi_n)\langle\psi_{n'}|\hat{U}^\dagger\hat{n}_a\hat{U}-\hat{n}_a|\psi_n\rangle. \tag{2.27}$$

If each on-site state is not entangled or superposed with any other on-site state, then $\mathcal{R}$ can be written in factorized form, $\mathcal{R}(\psi_{n'},\psi_n)=\mathcal{C}(\psi_{n'})\mathcal{C}(\psi_n)$. In this case, Eq. (2.27) is simplified,

$$\Omega_a^{\text{meso}}=\langle\psi|\hat{U}^\dagger\hat{n}_a\hat{U}-\hat{n}_a|\psi\rangle, \tag{2.28}$$

where the coefficients $\mathcal{C}(\psi_n)$ specify any local superposition and entanglement

$$|\psi\rangle\equiv\sum_{\psi_n}\mathcal{C}(\psi_n)|\psi_n\rangle. \tag{2.29}$$

Then using Eq. (2.22), the lattice-Boltzmann equation for the quantum lattice-gas system becomes a local equation that can be easily simulated on a classical computer [7,8].

#### *3. The approach to steady-state equilibrium*

The system is said to be in *steady-state equilibrium* (which may also be called *thermodynamic equilibrium*) when the system ket $|\Psi^{\text{eq}}(t)\rangle$ is an eigenvector, with unity eigenvalue, of the collision operator $\hat{C}$,

$$\hat{C}|\Psi^{\text{eq}}\rangle\equiv|\Psi^{\text{eq}}\rangle. \tag{2.30}$$

The value of the probability of occupancy (2.11) is then determined from $|\Psi^{\text{eq}}\rangle$ as

$$f_a^{\text{eq}}(\vec{x},t)=\langle\Psi^{\text{eq}}(t)|\hat{n}_\alpha|\Psi^{\text{eq}}(t)\rangle. \tag{2.31}$$

Notice by the definition (2.30) for steady-state equilibrium, the collision term (2.20) in the lattice-Boltzmann equation vanishes,

$$\Omega_a^{\text{meso}}(|\Psi^{\text{eq}}\rangle)=0. \tag{2.32}$$

Therefore, at steady-state equilibrium, the occupancy probabilities are unchanging over time. That is, $|\Psi^{\text{eq}}\rangle$ is the ground state of the system. The distribution along the momentum directions of the particle occupancies are uniform, so the local configurations are perfectly symmetric, and $\Omega_a^{\text{meso}}$ cannot cause any further changes.

## III. NUMERICAL TREATMENT

### A. Methodology

#### *1. Universal two-qubit gate*

In this section, I write a two-qubit universal gate in terms of the creation and annihilation operators of the second quantized formulation of quantum mechanics. A classic text on second quantization is by Fetter and Walecka [16]. For our purposes, the two-qubit gate is a member of the special unitary group SU(2); I neglect the overall phase factor because this does not affect the quantum lattice-gas dynamics. If $\hat{U}$ is a member of SU(2), it can be parametrized using three real numbers $\xi$, $\zeta$, and $\theta$ as follows:

$$\hat{U}\equiv\begin{pmatrix}e^{i\xi}\cos\theta & -e^{i\zeta}\sin\theta\\ -e^{-i\zeta}\sin\theta & -e^{-i\xi}\cos\theta\end{pmatrix}. \tag{3.1}$$

Let $\hat{a}_\alpha^\dagger$ and $\hat{a}_\alpha$ denote the creation and annihilation operators for $\alpha$th spin of a fermionic quantum spin system. Then the spin-$\frac{1}{2}$ creation and annihilation operators satisfy the anticommutation relations

$$\{\hat{a}_\alpha,\hat{a}_\beta^\dagger\}=\delta_{\alpha\beta}, \tag{3.2}$$

$$\{\hat{a}_\alpha,\hat{a}_\beta\}=0,$$

$$\{\hat{a}_\alpha^\dagger,\hat{a}_\beta^\dagger\}=0.$$

The spin number operator $\hat{n}_i \equiv \hat{a}_\alpha^\dagger \hat{a}_\alpha$ has eigenvalues of 1 and 0 in the number representation when acting on a pure state, corresponding to the $i$th spin being up $s_z = \frac{1}{2}$ and down $s_z = -\frac{1}{2}$, respectively.

Consider a fermionic spin system with a total of $N$ spins whose system ket is denoted by $|\Psi\rangle$. Acting on this system ket with a unitary operator, we would like to entangle the two spin states, the states of the $\alpha$th and $\beta$th spins, according to the components of the special unitary matrix (3.1). Let $\Upsilon_{\alpha\beta}$ denote a square $2^N \times 2^N$ matrix that does this. I define $\Upsilon_{\alpha\beta}$ in terms of the multispin creation and annihilation operators as follows:

$$\Upsilon_{\alpha\beta} \equiv \mathbf{1} + e^{-i\zeta}\sin\theta\,\hat{a}_\beta^\dagger \hat{a}_\alpha + e^{i\zeta}\sin\theta\,\hat{a}_\alpha^\dagger \hat{a}_\beta - (1 + e^{i\xi}\cos\theta)\hat{n}_\alpha - (1 - e^{-i\xi}\cos\theta)\hat{n}_\beta - 2i\sin\xi\cos\theta\,\hat{n}_\alpha \hat{n}_\beta \tag{3.3}$$

for $\alpha \neq \beta$. Its matrix representation for a two-qubit system is

$$\Upsilon = \begin{pmatrix} 1 & 0 & 0 & 0 \\ 0 & e^{i\xi}\cos\theta & -e^{i\zeta}\sin\theta & 0 \\ 0 & -e^{-i\zeta}\sin\theta & -e^{-i\xi}\cos\theta & 0 \\ 0 & 0 & 0 & -1 \end{pmatrix}. \tag{3.4}$$

In Appendix B, I demonstrate why $\Upsilon_{\alpha\beta}$ is manifestly unitary and an appropriate formulation of a universal quantum gate.

In the special case when $\theta = \pi/2$, $\xi = 0$, and $\zeta = 0$, then $\Upsilon_{\alpha\beta}$ reduces an *interchange operator*

$$\chi_{\alpha\beta} \equiv \mathbf{1} + \hat{a}_\beta^\dagger \hat{a}_\alpha + \hat{a}_\alpha^\dagger \hat{a}_\beta - \hat{n}_\alpha - \hat{n}_\beta, \tag{3.5}$$

which is a NOT gate (see Appendix B).

### 2. Symbolic mathematics method

It is possible to simulate the exact quantum mechanical evolution of a quantum spin system using computational symbolic mathematics.[3] To test the quantum lattice-gas method, I implemented the algorithm using version 4 of MATHEMATICA [17]. Letting 1 and 0 represent spin up and spin down, respectively, the first step is to define a set of rules that encode the Fermionic anticommutation relations (3.2)

$$a^\dagger[0] = 1, \tag{3.6}$$

$$a^\dagger[1] = \aleph, \tag{3.7}$$

$$a^\dagger[\aleph] = \aleph, \tag{3.8}$$

$$a[0] = \aleph, \tag{3.9}$$

$$a[1] = 0, \tag{3.10}$$

$$a[\aleph] = \aleph, \tag{3.11}$$

where $\aleph$ is a symbol used to denote what I call the *null state* that accommodates Pauli exclusion and destruction on the vacuum. That is, the symbols $a^\dagger$ and $a$ represent the single-spin (or single qubit) creation and annihilation operators, respectively.

Next, all the basis states, in the number representation, are encoded by the symbol $\Psi[s]$, where $0 \leq s \leq 2^N - 1$, for a system with $N$ spins. That is, the states are binary encoded and labeled by $N$-bit integers. The state $\Psi[0]$ is called the *vacuum state*. The symbolic rules embodying the multiple-spin creation and annihilation operators are defined in terms of the single-spin rules

$$a^\dagger[\alpha, \Psi[s]] = \begin{cases} (-1)^{S_\alpha} a^\dagger[(s \wedge 2^\alpha) \Rightarrow \alpha] \\ 0, \qquad \text{if} \quad s = \aleph, \end{cases} \tag{3.12}$$

$$a[\alpha, \Psi[s]] = \begin{cases} (-1)^{S_\alpha} a[(s \wedge 2^\alpha) \Rightarrow \alpha] \\ 0, \qquad \text{if} \quad s = \aleph, \end{cases} \tag{3.13}$$

where $0 \leq \alpha \leq N-1$ and where the factor $(-1)^{S_\alpha}$ appearing in Eqs. (3.12) and (3.13) accounts for a phase change of $\pi$ radians induced by commuting spins. In the number representation each basis state is denoted by a ket $|n_1 n_2 \cdots n_\alpha \cdots n_N\rangle$, where each $n$ is either 1 (particle present) or 0 (no particle present). The phase factor $S_\alpha$ is defined by

$$S_\alpha = n_1 + n_2 + \cdots + n_{\alpha-1}. \tag{3.14}$$

The bitwise AND operation is denoted here by the symbol $\wedge$. The symbol $\Rightarrow$ denotes a bitwise barrel roll to the right. That is, "$s \Rightarrow j$" means shift the integer $s$ to the right by $j$ digits. Hence, the result of the operation "$(s \wedge 2^\alpha) \Rightarrow \alpha$" is either 1 or 0, depending on whether or not a particle occupies the $\alpha$th local state. Notice that the symbols $a^\dagger$ and $a$ are overloaded, so that when they are used with a single argument, that argument is interpreted as a spin value. If $a^\dagger$ and $a$ are used with two arguments, the first argument is interpreted as a spin-index and the second argument is interpreted as a ket.

Notice that these symbolic definitions of the multiple-spin creation and annihilation operators use the basis-state symbol $\Psi$ on the LHS of the rules, but $\Psi$ is not used at all on the RHS in the definition of the rules. Hence, it may seem that the use of the symbol $\Psi$ is superfluous here. However, this is not the case, because its use allows me to define the action of the creation and annihilation operators on a superposition of basis states in a recursive fashion:

$$a^\dagger[\alpha, A\Psi[s] + B] = A\, a^\dagger[\alpha, \Psi[s]] + a^\dagger[\alpha, B], \tag{3.15}$$

$$a[\alpha, A\Psi[s] + B] = A\, a[\alpha, \Psi[s]] + a[\alpha, B]. \tag{3.16}$$

Using this convention, it is possible, for example, to destroy a spin in local state $\alpha$ of a superposed state, say $\Psi[s_1] + \Psi[s_2]$, by directly supplying this state as the second argument. Then, Eq. (3.13) correctly expands out to

[3] I developed this symbolic method in 1991 at Brandeis University, see http://xyz.plh.af.mil/Papers/pdf/ae91.pdf

$$a[\alpha,\Psi[s_1]+\Psi[s_2]]=a[\alpha,\Psi[s_1]]+a[\alpha,\Psi[s_2]]. \tag{3.17}$$

If the special symbol $\Psi$ were not used, then one would get the wrong answer,

$$a[\alpha,s_1+s_2]=a[\alpha,s_3], \tag{3.18}$$

where $s_3$ is the numerical sum of $s_1$ and $s_2$. Of course, it is possible to use a special symbol in place of the plus sign to represent superimposed states. I have chosen not to do this. With the $\Psi$ symbol convention, MATHEMATICA can by default manipulate expressions involving the superposition of an arbitrary number of states and represent them in memory in a compact fashion. After the action of the collision operator (which is mathematically defined earlier in this paper and symbolically defined immediately below) on to a superposed state, the resulting new state in general has identical basis states that are repeated in the superposition, where each occurrence has a different amplitude. Using the $\Psi$ symbol convention, all these types of replications are automatically reduced down to the one term, since MATHEMATICA automatically adds coefficients of common terms.

Next, the multiple-spin number operator is defined as a composition of the multiple-spin creation and annihilation rules

$$n[\alpha,\Psi]=a^\dagger[\alpha,a[\alpha,\Psi]]. \tag{3.19}$$

With rules (3.12), (3.13), and (3.19), for the creation, annihilation, and number operators, it is then straightforward to implement the universal gate, Eq. (3.3), by composition:

$$\begin{aligned}U[s_1,s_2,\Psi]=\Psi&-Ca^\dagger[s_2,a[s_1,\Psi]]-Ba^\dagger[s_1,a[s_2,\Psi]]\\&+(A-1)n[s_{1a},\Psi]+(D-1)n[s_2,\Psi]\\&-(A+D)n[s_1,n[s_2,\Psi]],\end{aligned} \tag{3.20}$$

where the $c$ numbers $A$, $B$, $C$, and $D$ are components of an SU(2) matrix $\left(\begin{smallmatrix}A & B\\ C & D\end{smallmatrix}\right)$.

In the case of the quantum 1D3Px model, the collision operator mixes the on-site kets, $|011\rangle$ and $|100\rangle$. Three qubits are affected. I use a modified rule to directly handle this situation. The on-site collision operator for the 1D3Px quantum lattice gas is implemented by the following composition of universal gates:

$$\begin{aligned}U[s_{1a},s_{1b},s_2,\Psi]=\Psi&-Ca^\dagger[s_2,a[s_{1a},a[s_{1b},\Psi]]]\\&-Ba^\dagger[s_{1a},a^\dagger[s_{1b},a[s_2,\Psi]]]\\&-(1-A)n[s_{1a},n[s_{1b},\Psi]]\\&-(1-D)n[s_2,\Psi]\\&+(1-D)n[s_{1a},n[s_2,\Psi]]\\&+(1-D)n[s_2,n[s_{1b},\Psi]]\\&-(A-D)n[s_{1a},n[s_{1b},n[s_2,\Psi]]].\end{aligned} \tag{3.21}$$

The lattice-gas collision operator according to Eq. (2.7) for the $V=7\ell$ system is thus defined as a sevenfold composition

$$\begin{aligned}C[\Psi]=U[&20,21,19,U[17,18,16,U[14,15,13,U[11,12,10,\\&\times U[8,9,7,U[5,6,4,U[2,3,1,\Psi]]]]]]].\end{aligned} \tag{3.22}$$

This is actually handled recursively in the symbolic implementation, so $C$ works regardless of the size of the system.

The streaming operator for the quantum lattice gas is implemented using two rules, one to stream the right moving particles, denoted $S_+$, and the other to stream the left moving particles, denoted $S_-$. Note that the right moving particles occupy local states 2,5,8,11,14,17,20 and the left moving particles occupy local states 3,6,9,12,15,18,21. $S_+$ and $S_-$ are defined in terms of a sevenfold composition of interchange operators (3.5):

$$\begin{aligned}S_+[\Psi]=\chi[2,5,\chi[5,8,\chi[8,11,\chi[11,14,\chi[14,17,\\\times\chi[17,20,\Psi]]]]]],\end{aligned} \tag{3.23}$$

$$\begin{aligned}S_-[\Psi]=\chi[21,18,\chi[18,15,\chi[15,12,\chi[12,9,\chi[9,6,\\\times\chi[6,3,\Psi]]]]]].\end{aligned} \tag{3.24}$$

Again, these are handled recursively in the symbolic implementation, so the streaming operators work regardless of the size of the system. A global shift of particles is done by successive local interchanges of particles occupancies [18].

Finally, the evolution rule, denoted $E$, for the entire quantum system is the composition of the last three rules

$$E[\Psi]=C[S_+[S_-[\Psi]]]. \tag{3.25}$$

Any other compound rules that may be needed in a simulation can be defined in a similar fashion by composing predefined simpler rules. Therefore, beginning with a superpositon of basis states $\Phi(t)=\Sigma_s\phi_s\Psi[s]$ the dynamical evolution equation corresponding to Eq. (2.3) is

$$\Phi(t+\tau)=E[\Phi(t)], \tag{3.26}$$

where the result is a new superposition over a different set of basis states $\Phi(t+\tau)=\Sigma_{s'}\phi_{s'}\Psi[s']$.

### B. The 1D3Px model

#### 1. Classical version

Let us consider a simple lattice-gas model as a concrete example, called the *1D3Px lattice-gas model*, in this paper. This model was first studied by Qian in 1990 [19] and is referred to as Model I in his thesis. The lattice gas is one dimensional and has three bits per site, a rest particle with mass two and speed $\pm1$ particles with mass one. The mass and momentum at a lattice site is

$$m=2n_0+n_1+n_2 \quad \text{and} \quad p_x=n_1-n_2. \tag{3.27}$$

There are two local configurations both with $m=2$ and $p_x=0$: (1) $\{n_0,n_1,n_2\}=\{1,0,0\}$ and (2) $\{n_0,n_1,n_2\}=\{0,1,1\}$.

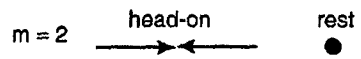


FIG. 1. Head-on collision in the 1D3Px lattice-gas model. The single equivalence class has $m=2$ and $p_x=0$.

These two configurations are members of the only collision set (which is called an *equivalence class*). An equivalence class has two or more members. Figure 1 illustrates the equivalence class of the 1D3Px model. Its two elements are the configuration of two head-on particles {011} and the configuration with a single rest particle {100}.

Because the total number of particles and the total momentum must be conserved, the collision part of the dynamics can only permute the local configurations. The collision equation, which is applied homogeneously across the lattice, can be expressed as in terms of a mapping function $U$ as follows:

$$s' = U(s), \tag{3.28}$$

where $U$ maps $2^B$ configurations to $2^B$ new configurations. For the simple 1D3Px lattice, $U$ is

$$U(\{011\}) = \{100\},$$

$$U(\{100\}) = \{011\}.$$

If a configuration $s$ is not a member of an equivalence class, then $U(s)=s$. In other words, if the incoming state is not a member of an equivalence class, then the outgoing state is set equal to the incoming state. To speed up a lattice-gas simulation, the mapping function $U$ may be precomputed before the simulation and accessed in *lookup table* fashion during the simulation.

In a computer implementation, it is convenient to use two arrays to simultaneously store the states $s$ and $s'$. Therefore, in Eq. (3.28), data in the array that stores the "incoming" state $s$ is transformed by the action of the lookup table $U$ (which is applied homogeneously over the entire array) and the output is written into the next array to store the new "outgoing" state $s'$.

It is conventional to write the collision rule in terms of the occupation variables $n_a=1$ or 0, which are Boolean values. The collision rule, expressed for an individual local state, is written

$$n_a'(\vec{x},t) = n_a(\vec{x},t) + \Omega_a(n_*), \tag{3.29}$$

where the collision term $\Omega_a(n_*)=\pm 1$ or 0. Writing $\Omega_a(n_*)$ with an asterisk subscript on $n_*$ denotes that the collision term for the $a$th local state depends on all the on-site local states. It is conventional to write the streaming rule in terms of $n_a$ also,

$$n_a(\vec{x}+\ell\hat{e}_a, t+\tau) = n_a'(\vec{x},t). \tag{3.30}$$

Combining Eqs. (3.29) and (3.30), the *microscopic transport equation* is therefore

$$n_a(\vec{x}+\ell\hat{e}_a, t+\tau) = n_a(\vec{x},t) + \Omega_a(n_*). \tag{3.31}$$

For the 1D3Px model, the lattice vectors are $\hat{e}_0=\vec{0}$, $\hat{e}_1=\hat{x}$, and $\hat{e}_2=-\hat{x}$ and the collision term is specified by the single function

$$\Omega = n_1 n_2 (1-n_0) - n_0 (1-n_1)(1-n_2), \tag{3.32}$$

where $\Omega_0=\Omega$ and $\Omega_{1,2}=-\Omega$. Then explicitly for the 1D3Px model, the microscopic transport equation (3.31) is

$$n_0(x, t+\tau) = n_0(x,t) + \Omega(x,t), \tag{3.33}$$

$$n_{1,2}(x\pm\ell, t+\tau) = n_{1,2}(x,t) - \Omega(x,t).$$

A lattice-Boltzmann equation describes the dynamics of the 1D3Px lattice-gas system at the mesoscopic scale. The mesoscopic average of the occupation variable $n_a(\vec{x},t)$ is the probability of occupancy

$$f_a(\vec{x},t) \equiv \langle n_a(\vec{x},t)\rangle. \tag{3.34}$$

Here, the angle brackets around a microscopic quantity denote its mesoscopic expectation value obtained by ensemble averaging. The kinetic transport equations are

$$f_0(x, t+\tau) = f_0(x,t) + \langle\Omega(x,t)\rangle, \tag{3.35}$$

$$f_{1,2}(x\pm\ell, t+\tau) = f_{1,2}(x,t) - \langle\Omega(x,t)\rangle.$$

To carry out a classical lattice-gas simulation at the mesoscopic scale, we can approximate $\Omega^{\text{meso}}(x,t)\equiv\langle\Omega(x,t)\rangle$ by a *mean-field* collision term, denoted $\Omega^{\text{mf}}(x,t)$, that neglect particle-particle correlations:

$$\langle\Omega(x,t)\rangle \simeq \Omega^{\text{mf}}(x,t) = f_1 f_2 (1-f_0) - f_0 (1-f_1)(1-f_2). \tag{3.36}$$

A statement of detailed balance can be written by setting the mean-field value of the collision term (3.36) to zero at equilibrium

$$\langle\Omega\rangle \simeq \Omega^{\text{mf}}(f_*^{\text{eq}}) = 0. \tag{3.37}$$

Therefore, the probability of occupancies satisfies the equation

$$f_0^{\text{eq}} = \frac{f_1^{\text{eq}} f_2^{\text{eq}}}{f_1^{\text{eq}} f_2^{\text{eq}} + (1-f_1^{\text{eq}})(1-f_2^{\text{eq}})}. \tag{3.38}$$

This equation, along with equations for the mass and momentum densities

$$\rho_{\text{O}} = 2f_0^{\text{eq}} + f_1^{\text{eq}} + f_2^{\text{eq}} \quad \text{and} \quad u_{x\text{O}} = f_1^{\text{eq}} - f_2^{\text{eq}}, \tag{3.39}$$

gives us a nonlinear system of three equations in five unknowns $f_0^{\text{eq}}$, $f_1^{\text{eq}}$, $f_2^{\text{eq}}$, $\rho_{\text{O}}$, and $u_{x\text{O}}$. Hence, it is possible to analytically solve for the occupation probabilities $f_0^{\text{eq}}$, $f_1^{\text{eq}}$, and $f_2^{\text{eq}}$ in terms of $\rho_{\text{O}}$ and $u_{x\text{O}}$. When the system is at rest at equilibrium, $p_x=0$, then $f_1^{\text{eq}}=f_2^{eq}=d$ and the probability of occupancy for the rest particle state is

$$f_0^{\mathrm{eq}}=\frac{d^2}{1-2d+2d^2}. \tag{3.40}$$

Using Eq. (3.36), the Jacobian of the collision $J_{ab} \equiv \partial\Omega_a^{\mathrm{mf}}/\partial f_b|_{f^{\mathrm{eq}}}$ is

$$J=\begin{pmatrix} -1+2d-2d^2 & \frac{(1-d)d}{1-2d+2d^2} & \frac{(1-d)d}{1-2d+2d^2} \\ 1-2d+2d^2 & \frac{(d-1)d}{1-2d+2d^2} & \frac{(d-1)d}{1-2d+2d^2} \\ 1-2d+2d^2 & \frac{(d-1)d}{1-2d+2d^2} & \frac{(d-1)d}{1-2d+2d^2} \end{pmatrix}. \tag{3.41}$$

The eigenvectors of $J$ are

$$|1\rangle=(2,1,1), \tag{3.42}$$

$$|2\rangle=(0,1,-1), \tag{3.43}$$

$$|3\rangle=\left(\frac{(1-2d+2d^2)^2}{d(d-1)},1,1\right). \tag{3.44}$$

The eigenvectors $|1\rangle$ and $|2\rangle$, corresponding to mass and momentum, span a two-dimensional hydrodynamic subspace. The remaining eigenvector $|3\rangle$ is a kinetic eigenvector, which in this case is density dependent. The eigenvalues of $J$ are

$$\lambda_1=0, \tag{3.45}$$

$$\lambda_2=0, \tag{3.46}$$

$$\lambda_3=\frac{1-2d+6d^2-8d^3+4d^4}{-1+2d-2d^2}. \tag{3.47}$$

Now using the lattice vectors $\hat{e}_0=0$, $\hat{e}_1=1$, and $\hat{e}_2=-1$, and the expression for $J$ given in Eq. (3.41), we set the secular determinant of the linearized Boltzmann equation equal to zero

$$[(e^{i(\ell_s\hat{e}_a\cdot\tilde{k}+\omega\tau)}-1)\delta_{ab}-J_{ab}]=0. \tag{3.48}$$

This allows us to solve for the dispersion relations for the lattice-gas system obeying what is called *generalized hydrodynamics*. Equation (3.48) is a result from the generalized hydrodynamics of classical lattice-gas systems previously worked out by Das, Bussemaker, and Ernst [20] and Grosfils, Boon, Brito, and Ernst [21]. Taking $\ell=\tau=1$, we get the following dispersion relation:

$$(1-2d+2d^2)e^{3\omega}-2[d-3d^2+4d^3-2d^4 +(1-3d+3d^2)\cos k]e^{2\omega} \tag{3.49}$$

$$+(1-2d)^2[1+2d(d-1)\cos k]e^{\omega}+4d^2(d-1)^2=0. \tag{3.50}$$

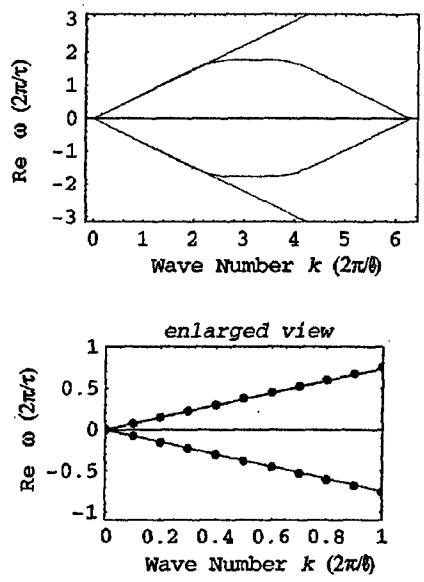


FIG. 2. The real part of the dispersion relation for the mesoscopic 1D3Px lattice gas in the long wavelength limit and mean-field limit at a reduced background density of $d=0.214\,286$.

This is a cubic equation in $e^{\omega}$, and it is analytically solvable. The only hydrodynamic mode is a damped sound wave $\omega(\vec{k})=\pm c_s k+i\Gamma(\rho)k^2$. Real and imaginary parts of the dispersion relations for the 1D3Px lattice-gas model are shown, respectively in Fig. 2 and Fig. 3. The real part of the dispersion relations indicates a sound mode [$\mathrm{Re}(\omega)\rightarrow\pm c_s k$ as $k\rightarrow 0$]. The imaginary part of the dispersion relation for the hydrodynamic mode is parabolic for small wave numbers, indicating viscous damping of the sound mode [$\mathrm{Im}(\omega)\rightarrow\Gamma k^2$ as $k\rightarrow 0$]. The sound damping constant $\Gamma$ approaches zero as the background mass density approaches zero [19]. That is, low-mass density waves can oscillate without viscous damping.

The real part of the dispersion relation for the sound mode for the 1D3Px lattice-gas model set with a background density of $d=6/4V$, with $V=7\ell$, is shown in Fig. 2. The real part of the dispersion relation indicates a sound mode [$\mathrm{Re}(\omega)\rightarrow\pm c_s k$ as $k\rightarrow 0$ where $c_s=0.74\ell/\tau$]. The data points, plotted as black circles, are solutions to the linearized Boltzmann equation in the mean-field limit. The curves with slope of $\pm c_s$ are numerical linear fits to the data. The imaginary part of the dispersion relation for the sound mode for

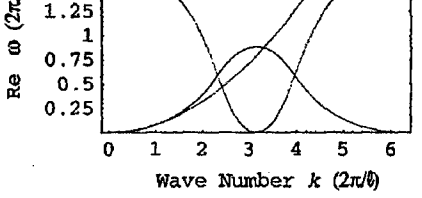


FIG. 3. The imaginary part of the dispersion relation for the mesoscopic 1D3Px lattice gas in the long wavelength limit and mean-field limit at a reduced background density of $d=0.214\,286$.

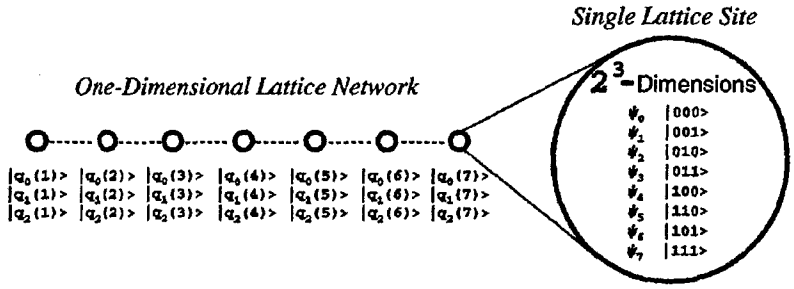


FIG. 4. A one-dimensional array of quantum computers with three qubits per node.

the 1D3Px lattice-gas model is shown in Fig. 3. The imaginary part of the dispersion relation indicates sound damping $[\mathrm{Im}(\omega)\to i\Gamma k^2$ as $k\to 0$ where $\Gamma=0.08\ell^2/\tau$. The parabola is a numerical fit to the data in the region of small $k<1$. The calculations shown in Figs. 2 and 3 were done with a mass density filling fraction of $d_{\bigcirc}=6/4V=0.214$, where a small system size of $V=7\ell$ is used. In this case, $k=2\pi/V=0.898$.

### 2. Quantum version

A hypothetical lattice-based quantum computer (with computational sites depicted as circles) arranged as a one-dimensional lattice is shown in Fig. 4. At each lattice site resides $B=3$ qubits in 1D in this example with $V=7\ell$ sites. The *on-site ket* $|\psi\rangle$ resides in a $2^B$-dimensional submanifold. The large circle on the right represents an expanded view of this on-site submanifold, which is denoted by $\mathcal{B}$. The basis states of $\mathcal{B}$ are shown in the number representation. Each site is coupled to its nearest neighboring sites by a mechanism allowing for the exchange of qubits. If the exchange mechanism retains all quantum entanglement (and thereby spreading it through the quantum computer), then the quantum computer is considered fully coherent. If the exchange mechanism is classical (destroying quantum entanglement by collapsing the wave function), then it is called a *type II quantum computer* (which is simply a large array of small quantum computers interconnected by a classical communication network).

The associated 1D3Px quantum lattice-gas model has three qubits per site, $|q_a\rangle=\alpha_a|0\rangle+\beta_a|1\rangle$ for $a=0,1,2$. The zeroth qubit represents a rest particle of mass two and the first and second qubits represent moving particles of speeds $\pm 1$, translating in the right and left going directions, respectively.

The $m=2$, $p_x=0$ equivalence class is spanned by the states $|100\rangle$ and $|011\rangle$. Collisional entanglement occurs only between these two states, $\xi|100\rangle+\chi|011\rangle$, where $\xi$ and $\chi$ are $c$ numbers. The on-site ket, $|\psi\rangle=|q_0\rangle\otimes|q_1\rangle\otimes|q_2\rangle$, is

$$\begin{aligned}|\psi\rangle=&\beta_0\beta_1\beta_2|111\rangle+\beta_0\beta_1\alpha_2|110\rangle+\beta_0\alpha_1\beta_2|101\rangle\\&+\beta_0\alpha_1\alpha_2|100\rangle+\alpha_0\beta_1\beta_2|011\rangle+\alpha_0\beta_1\alpha_2|010\rangle\\&+\alpha_0\alpha_1\beta_2|001\rangle+\alpha_0\alpha_1\alpha_2|000\rangle.\end{aligned}\tag{3.51}$$

The outgoing on-site ket $|\psi'\rangle=\hat{U}|\psi\rangle$ is

$$\begin{pmatrix}\beta_0\beta_1\beta_2\\ \beta_0\beta_1\alpha_2\\ \beta_0\alpha_1\beta_2\\ a\beta_0\alpha_1\alpha_2+b\alpha_0\beta_1\beta_2\\ c\alpha_0\beta_1\beta_2+d\alpha_0\beta_1\beta_2\\ \alpha_0\beta_1\alpha_2\\ \alpha_0\alpha_1\beta_2\\ \alpha_0\alpha_1\alpha_2\end{pmatrix}=\begin{pmatrix}1&0&0&0&0&0&0&0\\0&1&0&0&0&0&0&0\\0&0&1&0&0&0&0&0\\0&0&0&a&b&0&0&0\\0&0&0&c&d&0&0&0\\0&0&0&0&0&1&0&0\\0&0&0&0&0&0&1&0\\0&0&0&0&0&0&0&1\end{pmatrix}\begin{pmatrix}\beta_0\beta_1\beta_2\\ \beta_0\beta_1\alpha_2\\ \beta_0\alpha_1\beta_2\\ \beta_0\alpha_1\alpha_2\\ \alpha_0\beta_1\beta_2\\ \alpha_0\beta_1\alpha_2\\ \alpha_0\alpha_1\beta_2\\ \alpha_0\alpha_1\alpha_2\end{pmatrix},\tag{3.52}$$

where the local collision operator is the $8\times 8$ matrix with one $2\times 2$ block, which is a member of the U(2) unitary group satisfying

$$|a|^2+|b|^2=|c|^2+|d|^2=1,\tag{3.53}$$

$$ac^*+bd^*=a^*c+b^*d=0,\tag{3.54}$$

$$|a|^2+|c|^2=|b|^2+|d|^2=1,\tag{3.55}$$

$$ab^*+cd^*=a^*b+c^*d=0.\tag{3.56}$$

The quantum 1D3Px lattice gas obeys detailed balance because the collision operator $\hat{U}$ is a unitary matrix [8].

The mass and momentum densities for the quantum lattice-gas system are

$$\rho=2\langle q_0|\hat{n}|q_0\rangle+\langle q_1|\hat{n}|q_1\rangle+\langle q_2|\hat{n}|q_2\rangle,\tag{3.57}$$

$$u_x=\langle q_1|\hat{n}|q_1\rangle-\langle q_2|\hat{n}|q_2\rangle.\tag{3.58}$$

Viscous dissipation does not necessarily occur in quantum lattice-gas systems. Global entanglement of the wave func-

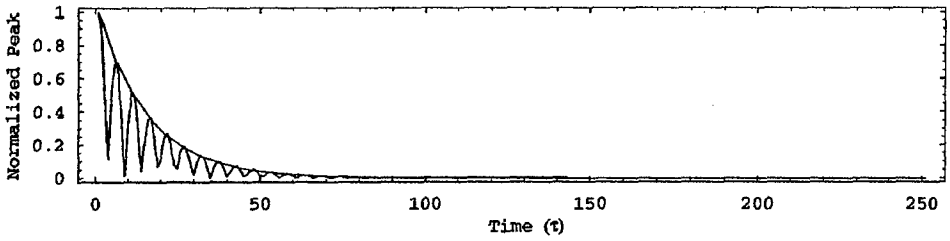


FIG. 5. Damping of a mass density wave for a system with $V-7$ sites in the classical 1D3Px model simulated using a mesoscopic Boltzmann equation with the collision term expressed in the mean-field approximation. The background density is $d_O=6/4V=0.214$. The ordinate is the absolute value of the amplitude of the mass-density wave divided by the peak amplitude of the initial perturbation.

tion significantly complicates the dispersion relations, which are determined by the following equation:

$$\mathrm{Det}\left[(e^{\ell e_a\cdot\hat{k}+\omega\tau}-1)\delta_{ab} - \frac{\partial\langle\Psi^{\mathrm{eq}}|(\hat{U}^{\dagger}\hat{n}_a\hat{U}-\hat{n}_a)\otimes\mathbf{1}\otimes\cdots\otimes\mathbf{1}|\Psi^{\mathrm{eq}}\rangle}{\partial f_b}\right]=0, \tag{3.59}$$

where $\Psi^{\mathrm{eq}}$ is the steady-state equilibrium wave funtion, which is the ground state of the system. I have explicitly written the collision operator, as in Eq. (2.23), in spatially separated form. In general, as described in Sec. II B1, $\alpha=\alpha_O+a$, where $\alpha_O$ is an index that refers to the first local state at some particular site in the system. According to the ordered numbering scheme used, $\alpha_O=0$ at the first site of the system, $\alpha_O=B$ at the second site, $\alpha_O=2B$ at the next site, and so on. Without loss of generality, in Eq. (3.59) we can assume we are working at the first site of the system where $\hat{n}_\alpha=\hat{n}_a\otimes\mathbf{1}\otimes\cdots\otimes\mathbf{1}$. In the classical case, $\hat{C}$ is a permutation matrix and the steady-state equilibrium wave function is a tensor product over the on-site kets

$$|\Psi^{\mathrm{eq}}\rangle=\bigotimes_{x=1}^{V}|\psi^{\mathrm{eq}}\rangle. \tag{3.60}$$

In turn, the on-site kets are formed by a tensor product over the individual qubits

$$|\psi^{\mathrm{eq}}\rangle=\bigotimes_{a=1}^{B}(\sqrt{f_a^{\mathrm{eq}}}|1\rangle+\sqrt{1-f_a^{\mathrm{eq}}}|0\rangle). \tag{3.61}$$

Finally, $f_{1,2}^{\mathrm{eq}}=d$ and $f_0^{\mathrm{eq}}=d^2/[d^2+(1-d)^2]$ according to Eq. (3.40). The Jacobian of the collision matrix element appearing in Eq. (3.59) is computable using Eqs. (3.60) and (3.61) [see Eq. (3.41) in Sec. III B 1]. In the quantum mechanical case, $|\Psi^{\mathrm{eq}}\rangle$ is not expressible as a tensor product state, and hence the Jacobian of the collision matrix element appearing in Eq. (3.59) becomes complicated.

### C. Simulations

#### 1. Classical simulation

A time history of the mass density wave for a small system with $V=7\ell$ sites is shown in Fig. 5. The exponential envelope is analytically determined by an analysis of the linearized lattice-Boltzmann equation in the mean-field limit (see Fig. 3). The predicted sound damping constant $\Gamma=0.08\ell^2/\tau$ is in excellent agreement with the simulation data.

Plotted in Fig. 6 are damping time constants of mass density waves in the classical 1D3Px lattice gas for different system sizes from $V=2\ell$ up to $V=256\ell$. The log-log plot shows the power-law behavior, known as *diffusive ordering*, typical of a lattice-gas system in the viscous regime. The power law in this case is $T=0.44V^2$, which is parabolic. Each circle is determined from a mesoscopic scale simulation that was initialized with a sinusoidal perturbation of $\delta\rho=0.04m/\ell$ from a uniform background mass density at half-filling, $\rho=2m/\ell$. The damping constant $\Gamma=\ell^2/T$ is determined from the envelope of the resulting standing wave $e^{-t/T}\cos\omega t$ (see Fig. 5). The mean-field estimates of the damping time constant are the circles. The line is a linear best fit to these estimates. The estimated damping constant deviates only slightly from power-law behavior at the smallest system sizes. This is an example of "fluidlike" behavior occurring in systems far below the continuum limit. The inset plot is a linear plot of the data for $V\leqslant 16$ and the parabola is the same diffusive-ordering power-law in the larger log-log plot.

#### 2. Quantum simulation

I have tested the quantum lattice-gas formalism described in this paper by carrying out exact numerical simulations of

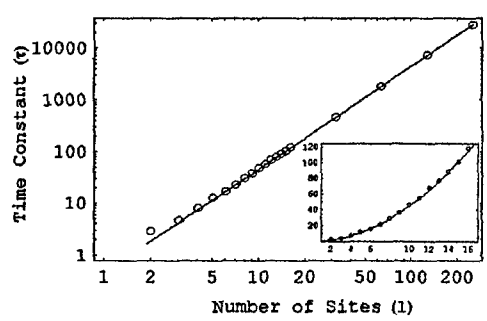


FIG. 6. Diffusive ordering in the classical 1D3Px model computing at the mesoscopic scale using the mean-field approximation.

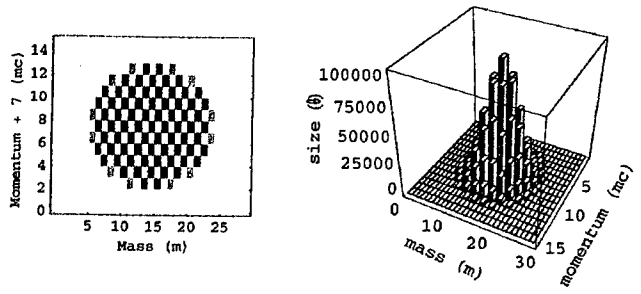


FIG. 7. Mass and momentum sectors of the 1D3Px lattice-gas model with $V=7\ell$ sites plotted versus the number of states per sector.

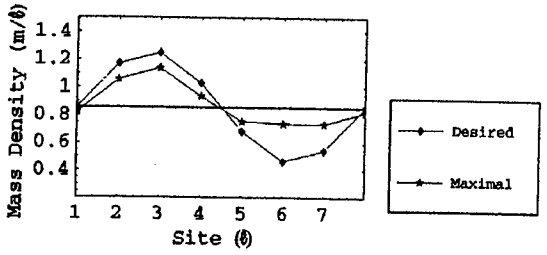


FIG. 8. Initial mass density sinusoidal perturbation in the quantum 1D3Px lattice gas for a small system size of $V=7\ell$ with periodic boundary conditions. The total number of qubits in the simulation is $BV=21$. The simulation is initialized with a sinusoidal perturbation in the $m=6$, $p_x=0$ mass-momentum sector with a peak amplitude of $\delta\rho\simeq 0.4$ from a uniform background mass density at $\rho_0=\frac{6}{28}=0.857$. So the fractional mass density variation is initially one part in two, which is an extremely large-scale fluctuation. The wavelength equals the system size. The initial mass density field is not exactly sinusoidal, because aside from the limitation of only $V=7\ell$ sites, it is produced by the interference of all 5376 in the $m=6$ and $p_x=0$ sector. An algorithm using Lagrangian multipliers maximizes the entropy of the resulting wave function and chooses all the amplitudes of the initial state.

a 1D3Px model, which is described in detail in Sec. III B 1. In this section, I present results obtained from the numerical simulation of a small system with $V=7\ell$ sites. I have used the symbolic numerical technique described above in Sec. III A 2. The principal finding is that the quantum lattice gas does not display viscous damping.

Since the evolution operator conserves mass and momentum, we can divide the Hilbert space into disjoint mass-momentum sectors. When the lattice-gas evolution operator maps a particular state residing in a mass-momentum sector to a new state, the new state must also reside in that same mass-momentum sector. The Hilbert space for the $V=7\ell$ system has over two million dimensions. The number of states within each mass-momentum sector of the $V=7\ell$ system are graphically illustrated in Fig. 7. The density plot on the left side of Fig. 7 clearly shows that the allowable mass-momentum sectors are all contained within a hexagonal boundary. The distribution for the number of available states within a mass-momentum sector is reflection symmetric about half-filling ($m=14$) and about zero momentum ($p_x=0$).

I have simulated the $V=7\ell$ system (with $BV=21$ globally entangled qubits) in the mass $m=6$ and momentum $p_x=0$ sector. In this mass-momentum sector, there are 5376 basis states. The goal of the numerical test was to measure the sound damping constant in the quantum 1D3Px model and compare the result to the mean-field estimate. The system was initialized with a sinusoidal perturbation of the mass density field, with a wavelength equaling the grid size of the periodic system ($\lambda=V$). All the states in the $m=6$, $p_x=0$ sector were superposed by choosing amplitudes in such a fashion that the entropy of the initial state is maximized, subject to the independent constraints of conservation of probability, mass, and momentum. The entropy function was taken to be

$$S=-\sum_{\alpha}\left[|c_\alpha|^2\ln|c_\alpha|^2+(1-|c_\alpha|^2)\ln(1-|c_\alpha|^2)\right], \tag{3.62}$$

where $c_\alpha$ is the amplitude of the ket $|\alpha\rangle$ in the $m=6$, $p_x=0$ mass-momentum sector. Given a particular desired profile of the mass density field, it is more difficult to construct an initial state that completely resides in only one sector than to use an initial state that spans the entire Hilbert space. However, it is computationally advantageous to limit the simulation to a single sector of the Hilbert space, so that memory allocation in the computer is kept at a manageable level. Figure 8 shows a maximized entropy state used in the test simulation presented in this section.

The data from the simulation run is presented in several ways. First, the peak amplitude of the mass density wave is recorded after every time step. The amplitude is normalized in such a fashion that at time $t=0$ it has unity value. In a viscous fluid with sound damping, the peak amplitude would oscillate and decay exponentially in time by the factor, $e^{-\Gamma t/\ell^2}\cos(2\pi c_s t/\ell)$, where $c_s$ is the sound speed and $\Gamma$ is a positive definite damping constant as is shown in Fig. 5. However, for the quantum 1D3Px model, the numerical result indicates $\Gamma$ may be zero for certain collision operators.

A time series history of the square of the peak amplitude is plotted in Fig. 9, using the same format as Fig. 5 for the classical 1D3Px model with the same grid size and initial condition. In the quantum simulation, the peak amplitude does not decay in time, unlike the results obtained in the classical lattice-Boltzmann simulations shown in Fig. 5. Initially, within the first couple of dozen time steps, the peak amplitude appears to decay, very much like it does in a classical microscopic simulation or lattice-Boltzmann simulation of the 1D3Px model. However, the amplitude does not continue to damp in subsequent time steps. The peak amplitude rises and falls. No damping is observed even after a thousand time steps. An expanded view of the first 250 time steps is shown underneath. Since the algorithm is unitary (and hence the collisions obey the principle of detailed balance) the dynamics is reversible.

In Fig. 10, these data are presented in scatter plot fashion, where the square of the normalized peak amplitude is plotted versus its first order time derivative. I used the following difference formula to approximate the time derivative:

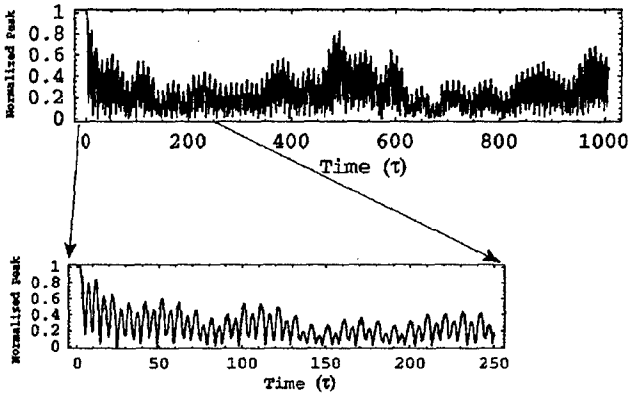


FIG. 9. Oscillations of a mass density wave in the quantum 1D3Px lattice gas for a system size of $V=7\ell$ in the $m=6$ and $p_x=0$ sector. The ordinate is the absolute value of the amplitude of the mass-density wave divided by the peak amplitude of the initial perturbation.

$$\frac{\partial \rho^2(x,t)}{\partial t} \simeq \frac{\rho^2(x,t-\tau)-\rho^2(x,t+\tau)}{2\tau}. \qquad (3.63)$$

The data appear randomly scattered, but is clustered along a "cone" corresponding to the speed of sound in the 1D3Px model, which the Boltzmann analysis of Sec. III B 1 predicts to be $c_s=0.74\ell/\tau$.

To obtain a more accurate estimate of the sound speed in the quantum 1D3Px simulation, a Fourier transform of the time series history of the mass density at a single site of the system was computed and the power spectrum $\rho^*_\omega(x)\rho_\omega(x)$ plotted (see the bottom plot of Fig. 11). The top plot shows

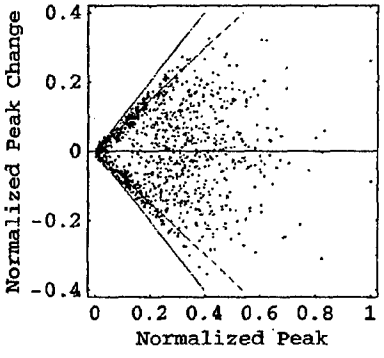


FIG. 10. Normalized peak (absolute value of the amplitude of the mass-density wave divided by the peak amplitude of the initial perturbation) versus the first derivative of the normalized peak of oscillations of a mass density wave in the quantum 1D3Px lattice gas for a system size of $V=7\ell$ in the $m=6$ and $p_x=0$ sector. We have plotted maximum speed curves corresponding the individual particle velocity, $c=\pm\ell/\tau$. As expected, all the data are contained within this "cone." In addition, we have plotted sound-speed curves corresponding to $c_s=\pm 0.74\ell/\tau$, which is analytically determined from a mean-field approximation of the system using the linearized lattice-Boltzmann equation. Most of the data is clustered around the sound-speed curves, and additional data points scattered within the "sound-speed cone" indicates randomness in the oscillation of the mass density wave.

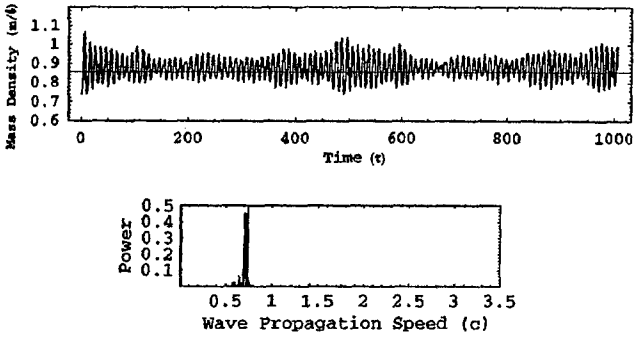


FIG. 11. Time history of the mass density at site $x=6\ell$ for a system with $V=7\ell$ sites plotted versus time. A discrete Fourier transform of this time series data is taken to give $\rho^*_\omega(x)\rho_\omega(x)$. A peak in the power spectrum $|\rho_\omega|^2$ occurs at about $0.72\ell/\tau$, which is close to the expected sound speed. The abscissa is converted into unit of velocity, $c=\ell/\tau$, to show that there is a unique sound speed. The ordinate has units of $(m/\ell\times\tau)^2$.

the time series collected by measuring the fluctuation of the mass density field of the $V=7\ell$ quantum 1D3Px lattice-gas system. The signal, which is $\rho(6\ell,t)$, is measured at site $x=6\ell$. Plotted below is the power spectrum of the Fourier transform of the signal, which is $|\rho_\omega|^2$, versus sound speed (this is proportional to the oscillation frequeny, $c_s=\ell f$). A peak in the power spectrum occurs just below the mean-field approximation of sound speed, $c_s=0.74\ell/\tau$, which is plotted as the vertical bar. (See Fig. 2 for the mean-field value estimate of $c_s$.)

## IV. CONCLUSION

The main results of this paper are as follows.

The quantum mechanical wave equation is recast as a lattice-Boltzmann equation describing a quantum lattice-gas system.

The continuity and Navier-Stokes equations constitute a macroscopic effective field theory for the quantum lattice-gas system and quantum entanglement changes the value of the transport coefficients.

A symbolic math method was presented for simulating dynamical quantum systems.

With reversible microscopic-scale dynamics, a feature of classical lattices is that dissipation occurs at the macroscopic scale. However, viscous damping is not observed in simulations of the quantum 1D3Px lattice-gas model, which is also microscopically reversible.

The sound speed of mass density waves is the same as the classical value.

Given the memory and speed constraints of classical computers, today only small quantum lattice gas can be exactly simulated. I have performed many test simulations of the quantum 1D3Px model for system sizes ranging from $V=3\ell$ up to $V=7\ell$ and have included results from the $V=7\ell$ quantum simulation in the paper, since this was the largest computer run.

I do not wish to argue that results obtained for such a small system, with $V=7\ell$ sites, can give us too much insight about the true macroscopic behavior of the quantum

lattice gas, which is only well defined in the continuum limit. Further testing is required on larger systems and in two and three dimensions and will be presented in a subsequent paper. Yet, in the classical version of the model, hydrodynamiclike behavior is observed in very small systems (see Figs. 5 and 6). The type of behavior found in the small $V=7\ell$ quantum lattice-gas system may also occur for larger systems. So, quantum lattice gases of multiple grid sizes should be simulated. To this end, a compiled version of quantum lattice-gas code is being developed in FORTRAN 90 and will be run on available supercomputers.

The issue of the similarity or distinction between particle-particle correlations (as occurs in classical lattice gases) and quantum entanglement (as occurs in quantum lattice gases) has not been addressed in this paper. Yet, this is an issue that can be studied using quantum lattice-gas simulations.

## ACKNOWLEDGMENTS

I would like to thank Bruce Boghosian for many helpful discussions about classical and quantum lattice gases, in particular, his suggestion to use a maximal entropy state as the initial state of the quantum lattice-gas simulation. This allowed me to constrain the quantum dynamics to a single mass-momentum sector of the full Hilbert space, and thereby speed up the symbolic computation. In the lattice-gas and lattice-Boltzmann literature, differential notation is applied to lattice-based mesoscopic fields with the understanding that the system is being analyzed in the continuum limit. This is usually not clearly explained, and may cause some confusion. I would like to acknowledge Hugh Pendleton for suggesting not to indiscriminately use differential point-form notion when describing the lattice-gas system at the mesoscopic space-time scale, since the mesoscopic-scale superlattice is discrete after either coarse-grain or ensemble averaging.

## APPENDIX A: DERIVATION OF THE QUANTUM LATTICE-GAS TRANSPORT EQUATION IN THE CONTINUUM LIMIT

In this appendix, I would like to rederive the transport equation (2.19) for the quantum lattice-gas system. The derivation given here is carried out in the continuum limit (imagine a space-time lattice with infinite resolution as the cell size vanishes). All the usual restrictions arising from the discretization of the microscopic quantities are temporarily removed. A particle can exist at any point in space and time, and it can also have any momentum $\vec{p}=m\vec{v}$. The only assumption I make here is that I can still decompose the space time into an ordered set of local states, which in this case is infinite but denumerable. That is, I imagine there are an infinite number of local states at each point in space ($B=\infty$), one corresponding to every possible particle momentum. Since the number of points in the space is also infinite ($V=\infty$), the total number of local states are doubly infinite ($N=BV=\infty^2$). Nevertheless, I assume the local states are well ordered and denumerable.

The probability of finding a particle with momentum $\vec{p}$ in the $\alpha$th local state located at position $\vec{x}$ given by Eq. (2.11) is the following matrix element:

$$f(\vec{x},\vec{p},t)\equiv\langle\Psi(t)|\hat{n}_\alpha|\Psi(t)\rangle. \tag{A1}$$

I assume $f(\vec{x},\vec{p},t)$ is a continuous and differentiable mesoscopic field quantity. For the moment, suppose the $\alpha$ is the local state of an "incoming" particle, preceding a possible collision event. I still want to imagine the particle dynamics divided into mutually exclusive events (collision followed by streaming) repeated in stepwise fashion *ad infinitum*. Next, the probability of finding a particle in the local state $\alpha'$, corresponding to momentum $\vec{p}'$ at position $\vec{x}'=\vec{x}+(\tau/m)\vec{p}'$, is expressed by the matrix element

$$f(\vec{x}+(\tau/m)\vec{p}',\vec{p}',t+\tau)\equiv\langle\Psi(t+\tau)|\hat{n}_{\alpha'}|\Psi(t+\tau)\rangle. \tag{A2}$$

Suppose $\alpha'$ is the local state of the "outgoing" particle. Then, a basic definition of the total time derivative of $f(\vec{x},\vec{p},t)$ is the following ratio:

$$\frac{df(\vec{x},\vec{p},t)}{dt}\equiv\lim_{\tau\to0}\frac{f(\vec{x}+(\tau/m)\vec{p}',\vec{p}',t)-f(\vec{x},\vec{p},t)}{\tau}, \tag{A3}$$

or, in terms of the matrix elements, it is

$$\frac{df(\vec{x},\vec{p},t)}{dt}=\lim_{\tau\to0}\frac{\langle\Psi(t+\tau)|\hat{n}_{\alpha'}|\Psi(t+\tau)\rangle-\langle\Psi(t)|\hat{n}_\alpha|\Psi(t)\rangle}{\tau}. \tag{A4}$$

This is the seed of a Boltzmann equation for particle transport and the RHS of this equation constitutes the collision term, although this may not appear quite obvious at this point in the development. In the following development, I shall interpret the collision term and rewrite it so that it explicitly depends only on $\hat{n}_\alpha$ at position $\vec{x}$ and $|\Psi(t)\rangle$. In so doing, we shall see how the collision dynamics is inherently encoded in this expression.

First, we add zero to the RHS of the above equation to write the collision term in two parts, explicitly separating the total change into "temporal-change" and "spatial-change" parts, as follows:

$$\frac{df(\vec{x},\vec{p},t)}{dt}=\lim_{\tau\to0}\frac{\langle\Psi(t+\tau)|\hat{n}_{\alpha'}|\Psi(t+\tau)\rangle-\langle\Psi(t)|\hat{n}_{\alpha'}|\Psi(t)\rangle}{\tau}+\lim_{\tau\to0}\frac{\langle\Psi(t)|\hat{n}_{\alpha'}|\Psi(t)\rangle-\langle\Psi(t)|\hat{n}_\alpha|\Psi(t)\rangle}{\tau}. \tag{A5}$$

From the time-displacement operation, $e^{\tau\partial/\partial t}f(\vec{x},\vec{p},t)=f(\vec{x},\vec{p},t+\tau)$, we see that the first term on the RHS of the above equation is a partial derivative with respect to time

$$\frac{\partial f(\vec{x}+(\tau/m)\vec{p},\vec{p},t)}{\partial t}+O(\mathrm{Sh}^2)=\lim_{\tau\to 0}\frac{\langle\Psi(t+\tau)|\hat{n}_{\alpha'}|\Psi(t+\tau)\rangle-\langle\Psi(t)|\hat{n}_{\alpha'}|\Psi(t)\rangle}{\tau}. \tag{A6}$$

The Stouhal number, Sh, is defined as the ratio of the mean-free time to the characteristic length scale (Sh$=\tau/t$). Similarly, from the space-displacement operation, $e^{\tau\vec{v}\cdot\nabla}f(\vec{x},\vec{p},t)=f(\vec{x}+\tau\vec{v},\vec{p},t)$, we see that the second term is a partial derivative with respect to position

$$\vec{v}\cdot\nabla f(\vec{x},\vec{p},t)+\frac{1}{2}(\vec{v}\cdot\nabla)^2 f(\vec{x},\vec{p},t)+O(\mathrm{Kn}^3)=\lim_{\tau\to 0}\frac{\langle\Psi(t)|\hat{n}_{\alpha'}|\Psi(t)\rangle-\langle\Psi(t)|\hat{n}_{\alpha}|\Psi(t)\rangle}{\tau}. \tag{A7}$$

The Knudsen number, Kn, is defined as the ratio of the mean-free path to the characteristic length scale (Kn $=\ell/L$). Therefore, we have the convective derivative

$$\frac{df(\vec{x},\vec{p},t)}{dt}=\frac{\partial f(\vec{x}+(\tau m/\vec{p}),\vec{p},t)}{\partial t}+\vec{v}\cdot\nabla f(\vec{x},\vec{p},t)+\frac{1}{2}(\vec{v}\cdot\nabla)^2 f(\vec{x},\vec{p},t)+O(\mathrm{Sh}^2,\mathrm{Kn}^3), \tag{A8}$$

composed of a local term and a nonlocal advection term. In the local term, it is technically correct (albeit unconventional) to explicitly write the partial time derivative's dependence on $\tau$, even though $\tau\to 0$. This is done to stress an equivalence with the matrix element formulation given by Eq. (A5).

Second, we rewrite the "local change" term. Since $|\Psi(t+\tau)\rangle=e^{i\hat{H}\tau/\hbar}|\Psi(t)\rangle$ and $e^{i\hat{H}\tau/\hbar}=1+i\hat{H}\tau/\hbar+O(\tau^2)$, we have

$$\langle\Psi(t+\tau)|\hat{n}_{\alpha'}|\Psi(t+\tau)\rangle=\langle\Psi(t)|\hat{n}_{\alpha'}|\Psi(t)\rangle+\frac{i\tau}{\hbar}\langle\Psi(t)|[\hat{n}_{\alpha'},\hat{H}]|\Psi(t)\rangle+O(\tau^2). \tag{A9}$$

Using this equation in conjuction with Eq. (A6), we have

$$\hbar\frac{\partial f\left(\vec{x}+\frac{\tau}{m}\vec{p},\vec{p},t\right)}{\partial t}=i\langle\Psi(t)|[\hat{n}_{\alpha'},\hat{H}]|\Psi(t)\rangle. \tag{A10}$$

This result is expected, since in quantum mechanics, the partial time derivative of an operator is found by calculating the commutator of that operator with the Hamiltonian. Using this result, the Boltzmann equation (A5) becomes

$$\frac{df(\vec{x},\vec{p},t)}{dt}=\frac{i}{\hbar}\langle\Psi(t)|[\hat{n}_{\alpha'},\hat{H}]|\Psi(t)\rangle+\lim_{\tau\to 0}\left\langle\Psi(t)\left|\frac{n_{\alpha'}-n_{\alpha}}{\tau}\right|\Psi(t)\right\rangle. \tag{A11}$$

Now the RHS no longer depends on $|\Psi(t+\tau)\rangle$ (so it is local in time), but it is still nonlocal in space because it depends on $\hat{n}_{\alpha'}$ as well. That is, if the RHS of the above equation were to depend only on $\hat{n}_{\alpha}$, then it would have "strictly local" form.

Third, using the fact that $e^{i\hat{H}\tau/\hbar}\equiv\hat{S}\hat{C}$, we can rewrite the commutator as

$$\frac{i}{\hbar}[\hat{n}_{\alpha'},\hat{H}]=\lim_{\tau\to 0}\frac{e^{-i\hat{H}\tau/\hbar}\hat{n}_{\alpha'}e^{i\hat{H}\tau/\hbar}-\hat{n}_{\alpha'}}{\tau}=\lim_{\tau\to 0}\frac{\hat{C}^\dagger\hat{S}^\dagger\hat{n}_{\alpha'}\hat{S}\hat{C}-\hat{n}_{\alpha'}}{\tau}. \tag{A12}$$

Now, $\hat{n}_{\alpha}$ and $\hat{n}_{\alpha'}$ are related by the similarity transformation (2.14), $\hat{n}_{\alpha}=\hat{S}^\dagger\hat{n}_{\alpha'}\hat{S}$, so the commutator reduces to

$$\frac{i}{\hbar}[\hat{n}_{\alpha'},\hat{H}]=\lim_{\tau\to 0}\frac{\hat{C}^\dagger\hat{n}_{\alpha}\hat{C}-\hat{n}_{\alpha'}}{\tau}. \tag{A13}$$

Inserting this into Eq. (A11) gives the final local form of the *quantum Boltzmann equation* for $f(\vec{x},\vec{p},t)$, which is

$$\frac{df(\vec{x},\vec{p},t)}{dt}=\lim_{\tau\to 0}\frac{1}{\tau}\langle\Psi(t)|\hat{C}^\dagger\hat{n}_{\alpha}\hat{C}-\hat{n}_{\alpha}|\Psi(t)\rangle. \tag{A14}$$

Notice that the collision term depends only on the wave function evaluated at time $t$ and the occupancy of the $\alpha$th local state located at position $\vec{x}$. However, if there exists quantum superposition between particles at different points in space, then $|\Psi(t)\rangle$ cannot be written in separable tensor product form over the spatial points. So in this case, the collision term is "nonlocal." Hence, when I say the lattice-Boltzmann equation is local in form, I mean this in a pseudo-classical sense, barring nonlocal quantum entanglements: And this is why I said in the introduction of this paper that the lattice-Boltzmann equation, which accounts for global entanglement through the collision process, is an exact reformulation of the many-body Schrödinger equation.

There is one more point to make in this appendix. From the basic definition (A3) for the total time rate of change of $f(\vec{x},\vec{p},t)$, we see that Eq. (A14) can be written as the following "finite-difference" equation

$$f(\vec{x}+(\tau/m)\vec{p}',\vec{p}',t)=f(\vec{x},\vec{p},t)+\langle\Psi(t)|\hat{C}^{\dagger}\hat{n}_{\alpha}\hat{C}-\hat{n}_{\alpha}|\Psi(t)\rangle. \tag{A15}$$

This is the lattice-Boltzmann equation [see Eq. (2.19) in Sec. II B 2]. It is important to note that the Boltzmann equation is still an exact representation of the particle dynamics, even when expressed in finite-difference form. This is immediately obvious when the identity $\hat{n}_{\alpha}=\hat{S}^{\dagger}\hat{n}_{\alpha'}\hat{S}$ is inserted into the collision term, $\langle\Psi(t)|\hat{C}^{\dagger}S^{\dagger}\hat{n}_{\alpha'}\hat{S}\hat{C}-\hat{n}_{\alpha}|\Psi(t)\rangle$. Then, the lattice-Boltzmann equation becomes a simple identity

$$f(\vec{x}+(\tau/m)\vec{p}',\vec{p}',t)=f(\vec{x},\vec{p},t)+\langle\Psi(t+\tau)|\hat{n}_{\alpha'}|\Psi(t+\tau)\rangle - \langle\Psi(t)|\hat{n}_{\alpha}|\Psi(t)\rangle. \tag{A16}$$

In the case of a finite resolution lattice (used in a computational simulation of the quantum lattice-gas system), the lattice-Boltzmann equation is the appropriate formulation of the particle dynamics. However, the quantum Boltzmann equation (A14), in differentiable point form, becomes the appropriate formulation of the particle dynamics when talking about the system in the continuum limit.

## APPENDIX B: REPRESENTATION OF A TWO-QUBIT GATE FOR A 2-SPIN SYSTEM

In this appendix, we show that Eq. (3.3) is a manifestly unitary operator that entangles two qubits according to the SU(2) special unitary group. Let us consider a quantum spin system with only two spins. Then the Hilbert space is four dimensional, and we choose the following basis kets in the number representation:

$$|00\rangle=\begin{pmatrix}1\\0\\0\\0\end{pmatrix},\quad |10\rangle=\begin{pmatrix}0\\1\\0\\0\end{pmatrix},\quad |01\rangle=\begin{pmatrix}0\\0\\1\\0\end{pmatrix},\quad |11\rangle=\begin{pmatrix}0\\0\\0\\1\end{pmatrix}. \tag{B1}$$

In this basis, the creation operators are

$$\hat{a}_1^{\dagger}=\begin{pmatrix}0&0&0&0\\-1&0&0&0\\0&0&0&0\\0&0&-1&0\end{pmatrix},\quad \hat{a}_2^{\dagger}=\begin{pmatrix}0&0&0&0\\0&0&0&0\\1&0&0&0\\0&1&0&0\end{pmatrix}. \tag{B2}$$

Since $\hat{a}_1^{\dagger}$ and $\hat{a}_2^{\dagger}$ have real components, the annihilation operators are the transpose of the matrices given in Eq. (B2): $\hat{a}_1=(\hat{a}_1^{\dagger})^T$ and $\hat{a}_1=(\hat{a}_1^{\dagger})^T$. The universal gate operator is expressed in terms of the following five operators:

$$\hat{a}_1^{\dagger}\hat{a}_2=\begin{pmatrix}0&0&0&0\\0&0&-1&0\\0&0&0&0\\0&0&0&0\end{pmatrix},\quad \hat{a}_2^{\dagger}\hat{a}_1=\begin{pmatrix}0&0&0&0\\0&0&0&0\\0&-1&0&0\\0&0&0&0\end{pmatrix}, \tag{B3}$$

and

$$\hat{n}_1(\mathbf{1}-\hat{n}_2)=\begin{pmatrix}0&0&0&0\\0&1&0&0\\0&0&0&0\\0&0&0&0\end{pmatrix},$$

$$(\mathbf{1}-\hat{n}_1)\hat{n}_2=\begin{pmatrix}0&0&0&0\\0&0&0&0\\0&0&1&0\\0&0&0&0\end{pmatrix},$$

$$\mathbf{1}-\hat{n}_1-\hat{n}_2=\begin{pmatrix}1&0&0&0\\0&0&0&0\\0&0&0&0\\0&0&0&-1\end{pmatrix}. \tag{B4}$$

We can represent a block diagonal $4\times4$ unitary matrix in terms of these five operators as follows:

$$\begin{pmatrix}1&0&0&0\\0&A&B&0\\0&C&D&0\\0&0&0&-1\end{pmatrix}=A\hat{n}_1(\mathbf{1}-\hat{n}_2)-B\hat{a}_1^{\dagger}\hat{a}_2-C\hat{a}_2^{\dagger}\hat{a}_1 + D(\mathbf{1}-\hat{n}_1)\hat{n}_2+\mathbf{1}-\hat{n}_1-\hat{n}_2. \tag{B5}$$

When the $2\times2$ block is a member of SU(2) as given by Eq. (3.1), this expression for a unitary matrix becomes a representation of a universal gate given by Eq. (3.3).

In this appendix, we used a two-spin quantum system as an example system for illustrating how a universal gate can be expressed in terms of the multispin creation and annihilation operators. Although we used a two-spin system in this example, the procedure outlined here also works for a spin system with an arbitrary number of spins.

All permutations of single fermion states may be implemented by successive application of a "interchange operator" [22], here denoted by $\hat{\chi}_{\alpha\beta'}$, where the permutations occur between state $\alpha$ at site $\vec{x}$ and states $\beta'$ at site $\vec{x}'$

$$\hat{\chi}_{\alpha\beta'}=\hat{a}_{\alpha}^{\dagger}\hat{a}_{\beta'}+\hat{a}_{\beta'}^{\dagger}\hat{a}_{\alpha}+\mathbf{1}-\hat{a}_{\alpha}^{\dagger}\hat{a}_{\alpha}-\hat{a}_{\beta'}^{\dagger}\hat{a}_{\beta'}. \tag{B6}$$

This is a special case of the universal quantum gate, $\Upsilon_{\alpha\beta'}$ where $\theta=\pi/2$, $\xi=0$ and $\zeta=0$. The interchange operator correctly handles any necessary phase change due to the anticommutation relations (3.2).

[1] I. Bialynicki-Birula, Phys. Rev. D **49**, 6920 (1994).
[2] S. Succi, Physica D **69**, 327 (1993).
[3] S. Succi, Phys. Rev. E **53**, 1969 (1996).
[4] D.A. Meyer, J. Stat. Phys. **85**, 551 (1996).
[5] D.A. Meyer, Phys. Rev. E **55**, 5261 (1997).
[6] B.M. Boghosian and W. Taylor IV, Int. J. Mod. Phys. C **8**, 705 (1997).
[7] J. Yepez, Int. J. Mod. Phys. C **9**, 1587 (1999).
[8] J. Yepez, in *Quantum Computing and Quantum Communications*, edited by C. P. Williams, Lecture Notes in Computer Science (Springer-Verlag, Berlin, 1999), p. 480.
[9] R.P. Feynman, Optics News **11**, 11 (1985).
[10] D. Deutsch, Proc. R. Soc. London, Ser. A **425**, 73 (1989).
[11] A. Barenco, Proc. R. Soc. London, Ser. A **449**, 679 (1995).
[12] D.P. DeVincenzo, Phys. Rev. A **51**, 1015 (1995).
[13] A. Barenco *et al.*, Phys. Rev. A **52**, 3457 (1995).
[14] D. G. Cory, A. F. Fahmy, and T. F. Havel, in *Proceedings of the Fourth Workshop on Physics and Computation*, edited by T. Toffoli, M. Biafore, and J. L. Ao (New England Complex Systems Institute, 1996), pp. 87–91.
[15] N. Gershenfeld and I.L. Chuang, Science **275**(1), 350 (1997).
[16] A. L. Fetter and J. D. Walecka, *Quantum Theory of Many-Particle Systems* (McGraw-Hill, New York, 1971), p. 601.
[17] S. Wolfram, *The Mathematica Book*, 4th ed. (Cambridge University Press, Cambridge, England, 1999).
[18] J. Yepez, Am. Math. Soc. **6**, 261 (1996).
[19] Y. H. Qian, Ph.D. thesis, Departement De Physique, Universite De Paris, L'Ecole Normale Superieure, 1990 (unpublished).
[20] S. Das, H. Bussemaker, and M. Ernst, Phys. Rev. E **48**, 245 (1993).
[21] P. Grosfils, J.-P. Boon, R. Brito, and M.H. Ernst, Phys. Rev. E **48**, 2655 (1993).
[22] J. Yepez, Physics Ph.D. Program, Brandeis University, 1991 (unpublished).

# REPORT DOCUMENTATION PAGE

Form Approved
OMB No. 0704-0188



**1. REPORT DATE** *(DD-MM-YYYY)*
17-8-2005

REPRINT

**4. TITLE AND SUBTITLE**
A Quantum Lattice-Gas Model for Computational Fluid Dynamics

**5a. CONTRACT NUMBER**

**5b. GRANT NUMBER**

**5c. PROGRAM ELEMENT NUMBER**
61102F

**6. AUTHOR(S)**
Jeffrey Yepez

**5d. PROJECT NUMBER**
2304

**5e. TASK NUMBER**
0T

**5f. WORK UNIT NUMBER**
B1

**7. PERFORMING ORGANIZATION NAME(S) AND ADDRESS(ES)**
Air Force Research Laboratory/VSBYA
29 Randolph Road
Hanscom AFB MA 01731-3010

**8. PERFORMING ORGANIZATION REPORT NUMBER**
AFRL-VS-HA-TR-2005-1091

**9. SPONSORING / MONITORING AGENCY NAME(S) AND ADDRESS(ES)**

**10. SPONSOR/MONITOR'S ACRONYM(S)**

**11. SPONSOR/MONITOR'S REPORT NUMBER(S)**

**12. DISTRIBUTION / AVAILABILITY STATEMENT**
Approved for Public Release; Distribution Unlimited.

**13. SUPPLEMENTARY NOTES**
REPRINTED FROM: PHYSICAL REVIEW E, Vol 63, 046702, 2001
doi: 10.1103/PhysRevE.63.046702

**14. ABSTRACT**

Quantum-computing ideas are applied to the practical and ubiquitous problem of fluid dynamics simulation. Hence, this paper addresses two separate areas of physics: quantum mechanics and fluid dynamics (or specifically, the computational simulation of fluid dynamics). The quantum algorithm is called a *quantum lattice gas*. An analytical treatment of the microscopic quantum lattice-gas system is carried out to predict its behavior at the mesoscopic scale. At the mesoscopic scale, a lattice Boltzmann equation with a nonlocal collision term that depends on the entire system wave function, governs the dynamical system. Numerical results obtained from an exact simulation of a one-dimensional quantum lattice model are included to illustrate the formalism. A symbolic mathematical method is used to implement the quantum mechanical model on a conventional workstation. The numerical simulation indicates that classical viscous damping is not present in the one-dimensional quantum lattice-gas system.

**15. SUBJECT TERMS**
Quantum lattice gas  Quantum mechanics  Fluid dynamics
Mesoscopic scale

| **16. SECURITY CLASSIFICATION OF:** | | | **17. LIMITATION OF ABSTRACT** | **18. NUMBER OF PAGES** | **19a. NAME OF RESPONSIBLE PERSON** |
|---|---|---|---|---|---|
| | | | | | Jeffrey Yepez |
| **a. REPORT** | | **c. THIS PAGE** | SAR | | **19b. TELEPHONE NUMBER** *(include area code)* |
| UNCLAS | UNCLAS | UNCLAS | | | 781-377-5957 |